Cytotherapy, 2012 ; Early Online: 1–10

informa
healthcare

Human umbilical cord provides a significant source of unexpanded mesenchymal stromal cells

AKIE KIKUCHI-TAURA[1,2], AKIHIKO TAGUCHI[1], TAKAYOSHI KANDA[3], TAKAYUKI INOUE[2], YUKIKO KASAHARA[1], HARUKA HIROSE[1], IORI SATO[2], TOMOHIRO MATSUYAMA[4], TAKAYUKI NAKAGOMI[4], KENICHI YAMAHARA[1], DAVID STERN[5], HIROYASU OGAWA[2] & TOSHIHIRO SOMA[2]

[1]*Department of Regenerative Medicine, National Cerebral and Cardiovascular Center, Osaka, Japan,* [2]*Division of Hematology, Department of Internal Medicine, Hyogo College of Medicine, Hyogo, Japan,* [3]*Department of Perinatal Medicine, Osaka Minami Medical Center, Osaka, Japan,* [4]*Institute for Advanced Medical Sciences, Hyogo College of Medicine, Hyogo, Japan, and* [5]*Executive Dean's Office, University of Tennessee, Tennessee, USA*

Abstract

Background aims. Human mesenchymal stromal cells (MSC) have considerable potential for cell-based therapies, including applications for regenerative medicine and immune suppression in graft-versus-host disease (GvHD). However, harvesting cells from the human body can cause iatrogenic disorders and *in vitro* expansion of MSC carries a risk of tumorigenesis and/or expansion of unexpected cell populations. *Methods.* Given these problems, we have focused on umbilical cord, a tissue obtained with few ethical problems that contains significant numbers of MSC. We have developed a modified method to isolate MSC from umbilical cord, and investigated their properties using flow cytometry, mRNA analysis and an *in vivo* GvHD model. *Results.* Our study demonstrates that, using umbilical cord, large numbers of MSC can be safely obtained using a simple procedure without *in vitro* expansion, and these non-expanded MSC have the potential to suppress GvHD. *Conclusions.* Our results suggest that the combined banking of umbilical cord-derived MSC and identical cord blood-derived hematopoietic stem cell banking, where strict inspection of the infectious disease status of donors is performed, as well as further benefits of HLA-matched mesenchymal cells, could become one of the main sources of cells for cell-based therapy against various disorders.

Keywords: *cell banking, graft-versus-host disease, mesenchymal stromal cells, umbilical cord*

Introduction

Mesenchymal stromal cells (MSC) can be obtained from various tissues, including bone marrow (1), adipose tissue (2), trabecular bone (3), synovium (4), pancreas (5), lung, liver, spleen (6), peripheral blood (7), cord blood (8), amniotic fluid and umbilical cord (9–11). MSC include multiple cell types that have the capacity to differentiate into neurons, adipocytes, cartilage, skeletal muscle, hepatocytes and cardiomyocytes, under appropriate conditions across embryonic germ layers (2,12). Cell-based therapies using MSC have been initiated in patients with arthrosis (13), corneal disorders (14), stroke (15) and chronic heart failure (16). MSC are also used to suppress graft-versus-host disease (GvHD) in patients after allogeneic hematopoietic stem cell transplantation, and co-transplantation of hematopoietic cells and MSC to enhance engraftment has provided promising results (17). To broaden the indications for use of MSC against multiple disorders, cell banking with HLA-typing would be desirable.

Although MSC can be obtained from a range of organs, the iatrogenic risks associated with harvesting cells from the human body cannot be denied, particularly with harvesting from the large number of individuals required to establish a cell bank. In contrast, harvesting of cells from umbilical cord carries little risk to the donor, and MSC have been identified in placenta (18), amniotic fluid (19), umbilical cord blood (20) and the umbilical cord itself (21). Furthermore, the omission of *in vitro* expansion offers significant benefits for cell banks with large numbers of samples. The present study focused on the umbilical cord, because of the relative ease of cleaning the tissue before harvest and subsequent isolation of the cells. The umbilical cord is covered by

Correspondence: **Akihiko Taguchi,** Department of Regenerative Medicine, National Cerebral and Cardiovascular Center, 5-7-1 Fujishiro-dai, Suita, Osaka, Japan 565–8565. E-mail: taguchi@ri.ncvc.go.jp

(Received 2 June 2011; accepted 13 January 2012)

ISSN 1465-3249 print/ISSN 1477-2566 online © 2012 Informa Healthcare
DOI: 10.3109/14653249.2012.658911

an epithelium derived from the enveloping amnion and contains two arteries and one vein, all of which are surrounded by the mucoid connective tissue of Wharton's jelly. The main role of this jelly-like material is to prevent compression, torsion and bending of the enclosed vessels, which provide bidirectional blood flow between the fetal and maternal circulations. The network of glycoprotein microfibrils and collagen fibrils in Wharton's jelly has already been elucidated (22). The phenotypic stromal cells in Wharton's jelly are fibroblast-like cells (23), morphologically and immunophenotypically similar to MSC isolated from bone marrow (9,24,25). MSC from the umbilical cord have been shown to differentiate into adipocytes, osteocytes, neurons and insulin-producing cells (9,24–30). Carlin *et al.* (31) recently demonstrated embryonic transcription factors, such as octamer-binding transcription factor (Oct)-4, sex determining region Y-box (Sox)-2 and Nanog, in porcine umbilical cord matrix cells. These results indicate that umbilical cord-derived mesenchymal stem (UCMS) cells may represent a major source of cells for cell-based therapy. The present study demonstrates that large numbers of MSC can be obtained from umbilical cord using a simple procedure without *in vitro* expansion. Furthermore, UCMS isolated using this procedure are shown to suppress severe GvHD in a murine model.

Methods

All procedures for the isolation and differentiation of human UCMS cells were approved by the Osaka Minami Medical Center (Osaka, Japan). institutional review board and all volunteer donating mothers provided written informed consent. Animal experiments were carried out in accordance with the guidelines of the Animal Care Committee of Hyogo College of Medicine (Hyogo, Japan). Quantitative analyzes were conducted by an investigator who had been blinded to the experimental protocol, identities of animals and experimental conditions pertaining to the animals under study.

Isolation of UCMS cells

Human umbilical cords were obtained from patients delivered at full-term by Cesarean section ($n = 30$). After collection of cord blood as described previously (32), placenta and umbilical cord were placed into a sterilized bag and the following procedures were performed in a safety cabinet. In this study, we used only umbilical cord tissue for further experiments. Both ends of the umbilical cord (approximately 1 cm from each end) were cut and discarded with the placenta. The remaining umbilical cord was immersed and washed in 80% ethanol for 1 min, rinsed with sterile saline twice and cut into approximately 10-cm lengths. Cord blood and blood clots in the umbilical cord artery were removed by flushing twice, using a 20-G tip cut needle, sterile saline and 20-mL syringe. Then the umbilical cord segments were immersed and washed with 80% ethanol for 1 min, followed by two rinses with sterile saline. Next, the umbilical cord was cut into 2–4-cm lengths and the epithelial tissue was removed using sterilized scissors. The remaining tissue was incubated in an enzyme cocktail solution, containing 1 mg/mL hyaluronidase (Sigma-Aldrich, St Louis, MO, USA), 300 U/mL collagenase (Sigma-Aldrich) and 3 mM $CaCl_2$ (Wako Pure Chemical Industries, Osaka, Japan) in Dulbecco's modified Eagle's medium (DMEM) (Invitrogen, Carlsbad, CA, USA) for 2 h at 37°C with shaking (50 shakes/min; BR-21UM; Taitec, Saitama, Japan). After incubation, undigested vascular components were removed and the tissue solution was crushed with forceps and passed through 180- and 125-μm diameter stainless steel mesh (Tokyo Screen, Tokyo, Japan), followed by 70-μm diameter mesh (Becton Dickinson, Franklin Lakes, NJ, USA), to remove large pieces of unlysed tissue. The tissue solution was then collected by centrifugation (200 ***g*** for 5 min) and resuspended in phosphate-buffered saline (PBS). The latter washing procedure was performed twice. Next, the tissue solution was incubated with 0.5% trypsin–ethylenediamine tetraacetic acid. (EDTA) (Invitrogen) in PBS for 1 h at 37°C. After trypsinization, the tissue solution was neutralized with 2% fetal bovine serum (FBS) in DMEM and this washing procedure was performed twice. As a control, the conventional method of tissue preparation reported by Weiss *et al.* (29) was used to isolate UCMS cells. That procedure is similar to our own, the major difference being that we did not remove the umbilical artery from the umbilical cord before digestion with hyaluronidase and collagenase.

Flow cytometric analysis of UCMS cells

Antigens expressed by freshly isolated and *in vitro*-expanded and -differentiated umbilical cord-derived cells were investigated by multicolor flow cytometry. The expression of surface markers in 1×10^5 cells was analyzed. The characteristics of each antibody are listed in Table I. As a control, a non-immune isotype control (Beckman Coulter Orange County, CA, USA) was employed.

Expansion and in vitro *differentiation of UCMS cells*

To investigate the properties of isolated UCMS cells as MSC, cells were expanded *in vitro* as described previously (29). Briefly, 1×10^4 cells/cm^2 were plated in a low-serum media, containing 56% low-glucose DMEM (Invitrogen), 37% MCDB201

Table I. Antibodies for flow cytometry.

Antigen	Label	Manufacturer	Catalog number
CD11b	FITC	Beckman Coulter	IM1284
CD14	FITC	Beckman Coulter	IM0645
CD19	FITC	Beckman Coulter	IM1284
CD29	FITC	Beckman Coulter	6604105
CD31	FITC	BD	555445
CD34	PC7	Beckman Coulter	A21691
CD34	PC5	Beckman Coulter	A07777
CD38	FITC	Beckman Coulter	IM0775
CD44	PE[a]	Beckman Coulter	IM0845
CD45	FITC	Beckman Coulter	A07782
CD45	ECD	Beckman Coulter	A07784
CD73	Biotin[b]	BD	550256
CD90	PE	Beckman Coulter	IM1840
CD105	PE	Beckman Coulter	A07414
CD117	PE	Beckman Coulter	IM2732
CD133	PE	Miltenyi Biotec	130-080-901
GlycophorinA	PE	Beckman Coulter	IM2211
HLA-DR	FITC	BD	555560
vWF	FITC*	Beckman Coulter	IM0150

[a]Antibody was labeled with a Zenon Mouse IgG1 labeling kit (Invitrogen).
[b]Biotin-labeled antibody was detected by strept avidin–PC5.
FITC, fluorescein isothiocyanate; PE, phycoerythrin; PC, phycoerythrin-cyanin; ECD, phycoerythrin-TexasRED. BD, Becton Dickinson, Franklin Lakes, NJ, USA, Mitenyi Biotec; Bergisch Gladbach, Nordrhein-Westfalen, Germany

(Sigma-Aldrich), 2% FBS (StemCell Technologies, Vancouver, Canada), 1 × insulin-transferrin-selenium-X (ITS-X; Invitrogen), 1 × ALBU-Max I (Invitrogen), 1 × antibiotics-antimycotics (Invitrogen), 10 nM dexamethasone (Sigma-Aldrich), 50 μM ascorbic acid 2-phosphate (Sigma-Aldrich), 1 ng/mL epidermal growth factor (EGF; Peprotech, Rocky Hill, NJ, USA) and 10 ng/mL platelet-derived growth factor-BB (PDGF-BB; (R&D Systems, Minneapolis, MN, USA). After reaching 70–80% confluence, cells were replated at 20% confluence.

After cell expansion (passage 2), 70% confluent UCMS cells were differentiated into neuronal cells, adipocytes, osteocytes, chondrocytes, myoblasts, and pancreatic cells, as described previously (33–36). Briefly, prior to neuronal induction, UCMS cells were grown overnight in DMEM with 20% FBS (Invitrogen) and 10 ng/mL basic fibroblast growth factor (Peprotech). Cells were rinsed twice with PBS and incubated in DMEM with 100 μM butylated hydroxyanisole (BHA; Sigma-Aldrich), 10 μM forskolin (Sigma-Aldrich), 2% dimethyl sulfoxide (DMSO; Sigma-Aldrich), 5 U/mL heparin (Fuso Pharmaceutical Industries, Osaka, Japan), 5 nM K252a (Sigma-Aldrich), 25 mM KCl (Wako Pure Chemical Industries), 2 mM valproic acid (Sigma-Aldrich) and 1 × N2 supplement (Invitrogen). For differentiation into adipocytes, UCMS cells were incubated in DMEM with 1 μM dexamethasone, 0.5 mM 3-isobutyl-1-methlxanthine (Sigma-Aldrich), 1 μg/mL insulin (Sigma-Aldrich) and 100 μM indomethacin (Sigma-Aldrich). Differentiated cells were stained with Oil Red O (Sigma-Aldrich). For differentiation into osteocytes, UCMS cells were incubated in osteogenic differentiation medium in accordance with the manufacturer's protocol for 31 days (Invitrogen). Differentiated cells were stained with Alizarin Red S (Sigma-Aldrich). To investigate the potential formation of a chondrogenic pellet, UCMS cells were incubated in chondrogenic differentiation medium according to the manufacturer's protocol for 21 days (Invitrogen). Differentiated cell pellets were stained with Alcian Blue (Sigma-Aldrich) and cross-sections were studied. For differentiation into myoblasts, UCMS cells were initially incubated in DMEM with 2% FBS, 10 ng/mL EGF, 10 ng/mL PDGF-BB and 3 μM 5-azacytidine (Sigma-Aldrich) for 24 h. The medium was then changed to DMEM with 2% FBS, 10 ng/mL EGF and 10 ng/mL PDGF-BB. For differentiation into pancreatic cells, UCMS cells were cultured for 7 days in RPMI-1640 medium (Sigma-Aldrich) with 5% FBS and 10 mmol/L nicotinamide (Sigma-Aldrich). Cells were then cultured for an additional 5 days in the presence of 10 nM exendin 4 (Sigma-Aldrich).

Total RNA extraction and reverse transcriptase–polymerase chain reaction analysis

Total RNA was extracted from freshly isolated and *in vitro*-differentiated UCMS cells using RNeasy purification reagent (Qiagen, Hilden, Germany). Reverse transcriptase–polymerase chain reaction (RT-PCR) analysis was performed using a SuperScript One-Step RT-PCR System (Invitrogen) with 100 ng of tRNA. Sequences and annealing temperatures for each primer are described in Table II. The amplified cDNA was separated by electrophoresis through a 2% agarose gel, stained with ethidium bromide, and photographed under ultraviolet light.

GvHD model

Female B6C3F1 (recipient; C57BL/6 × C3H/He; H-$2^{b/k}$) and BDF1 (donor; C57BL/6 × DBA/2; H-$2^{b/d}$) mice between 8 and 12 weeks old were purchased from Japan SLC (Shizuoka, Japan). Mice were housed in sterile micro-isolator cages in a pathogen-free facility with *ad libitum* access to autoclaved food and hyperchlorinated drinking water. Donor bone marrow cells were harvested from tibiae and femurs by flushing with RPMI-1640 medium (Sigma-Aldrich). Recipient mice were lethally irradiated with 13 Gy total body irradiation (TBI; X-ray) split into two doses separated by 3 h. This amount of radiation and dose of infused donor cells has been shown to

Table II. Sequence of RT-PCR primers.

Gene	5′-primer	3′-primer	Temp. (°C)
Osteopontin	CTAGGCATCACCTGTGCCATACC	CAGTGACCAGTTCATCAGATTCATC	60
ALP	TCAGAAGCTCAACACCAACG	GTCAGGGACCTGGGCATT	51
Sox-9	ACATCTCCCCCAACGCCATC	TCGCTTCAGGTCAGCCTTGC	51
Aggrecan	TGCGGGTCAACAGTGCCTATC	CACGATGCCTTTCACCACGAC	51
PPARγ2	GCATTATGAGACATCCCCACTGC	CCTATTGACCCAGAAAGCGATTC	59
GFAP	CTGGGCTCAAGCAGTCTACC	AATTGCCTCCTCCTCCATCT	58
MAP-2	CTGCTTTACAGGGTAGCACAA	TTGAGTATGGCAAACGGTCTG	58
MyoD	GCTAGGTTCACGTTTCTCGC	GCGCCTTTATTTTGATCACC	58
Glucagon	GAGGGCTTGCTCTCTCTTCA	GTGAATGTGCCCTGTGAATG	57

ALP, alkaline phosphatase; GFAP, glial fibrillary acidic protein; MAP, microtubule-associated protein PPAR, peroxisome proliferator-activated receptor..

induce GvHD after hematopoietic stem cell transplantation (37). On the following day, donor-derived cells (1×10^7 bone marrow cells and 2×10^7 spleen cells) were suspended in 0.2 mL RPMI-1640 medium and transplanted via the tail vein into post-irradiation recipient mice. Soon after hematopoietic stem cell transplantation, 1×10^6 non-expanded and non-selected UCMS cells in 0.2 mL RPMI medium were transplanted via the tail vein. In the control group, the same amount of RPMI was infused via the tail vein. On day 7 after transplantation, the same number of non-expanded UCMS cells or RPMI medium alone was injected via the tail vein into treated mice or control mice, respectively. The severity of GvHD was evaluated using a scoring system incorporating five clinical parameters, as described previously (38): body weight; posture (hunching); mobility; fur texture; and skin integrity. Mice were evaluated and graded from 0 to 2 for each criterion. A clinical index was subsequently generated by summation of the five criteria scores (38). A score of 0–5 was defined as mild GvHD and a score of 6–10 or dead was defined as severe GvHD.

Statistical analysis

Statistical comparisons were performed using a Student's *t*-test or χ^2 test. For all experiments,

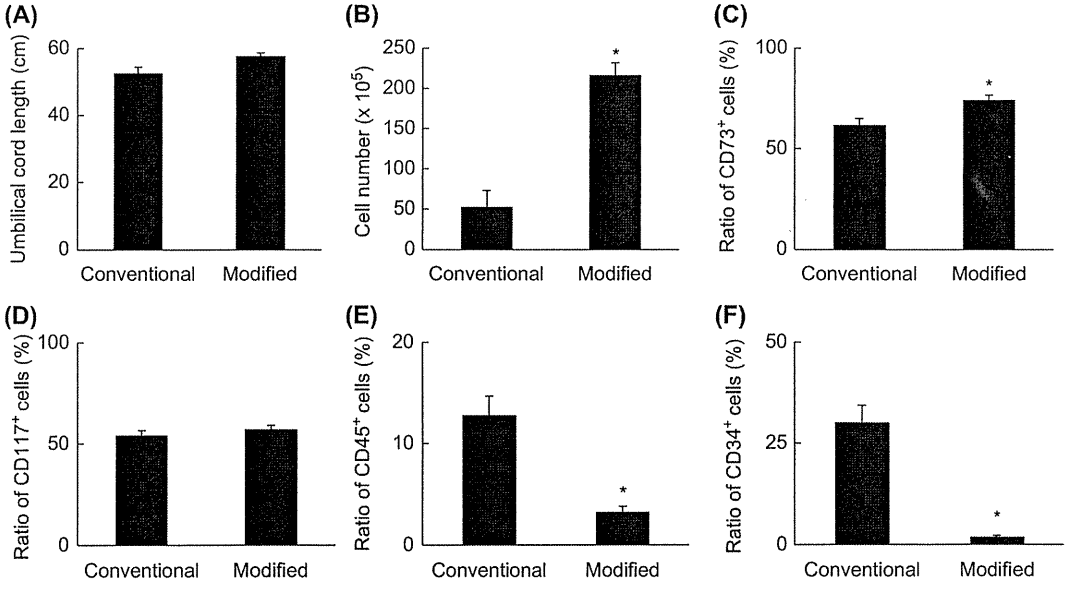

Figure 1. Cell numbers and characteristics of isolated MSC. No significant difference in the length of the umbilical cord was seen between groups (A). The total number of cells obtained with our modified method (216×10^5 cells) was more than 4-fold greater, compared with the conventional method (52×10^5 cells) (B). A significant increase in the ratio of cells expressing an MSC marker (CD73) was observed with the modified method (74.1%), compared with the conventional method (61.8%) (C). In contrast, no significant difference was observed in CD117-positive cells between modified (56.9%) and conventional methods (54.1%) (D). Contamination by cells from the hematopoietic lineage, expressing CD45 (E) and CD34 (F), was significantly decreased with the modified method (3.2% and 1.9%, respectively), compared with the conventional method (12.8% and 30.1%, respectively). *$P < 0.05$ versus conventional method.

values are reported as mean ± standard error of the mean. Values of $P < 0.05$ were considered statistically significant.

Results

Characterization of isolated UCMS cells

MSC were isolated from umbilical cord using either conventional methods (29) ($n = 12$) or our modified methodology ($n = 18$). Although no significant differences in the length of umbilical cords were observed (Figure 1A), more than four times as many cells were obtained using our method (Figure 1B). To investigate the characteristics of these cells, surface cell markers were analyzed by flow cytometry for CD73, as an MSC marker (Figure 1C); a significant increase in the ratio of CD73-positive MSC was observed using our method, compared with the conventional technique. In contrast, no significant difference in the ratio of cells positive for the stem cell marker CD117 was identified between groups (Figure 1D). Umbilical cord contains a range of cell types, including hemocytes and endothelial cells. To investigate the level of these cells in our final cell population, numbers of CD45- and CD34-positive cells were investigated by flow cytometry (CD45, Figure 1E; CD34, Figure 1F). We observed a significant reduction in contamination by endothelial cells using our modified methodology compared with the conventional technique.

To evaluate properties of freshly isolated umbilical cord-derived cells, cell surface markers were analyzed by multiple staining for cell-surface markers. As shown in Figure 2, only a small fraction of CD73-positive cells displayed hemocyte/hematopoietic cell markers, including anti-CD11b, CD14, CD19, CD34, CD38, CD45, CD133, GlycophorinA and HLA-DR. These results indicated that the CD73-positive cell fraction contained a low level of hemocyte or hematopoietic cells. To evaluate the presence of endothelial cells in the CD73-positive cell fraction, the expression of various endothelial cell markers, including CD31, CD34 and von Willebrand Factor (vWF), was investigated; the majority of CD73-positive cells were negative for these endothelial cell markers. To confirm our results, expression of CD90, a marker not present on endothelial cells (39), was evaluated; more than 95% of CD73-positive cells expressed CD90. These findings indicated little contamination by endothelial cells using our modified methodology and were consistent with the visual impression that most vascular components remained undigested after incubation with hyaluronidase and collagenase for 2 h.

Changes in cell-surface markers of isolated umbilical cord-derived cells after in vitro expansion

To evaluate further the character of the isolated cell population, freshly prepared umbilical cord-derived cells using our modified methodology were cultured up to passage 4. Expanded cells showed a spindle-shaped morphology (Figure 3A) that associated with common MSC. Analysis of cell-surface markers revealed that expression of CD44 (Figure 3B; a cell-surface glycoprotein involved in cell–cell interactions expressed by mesenchymal cells), CD105 (Figure 3C; a membrane glycoprotein expressed

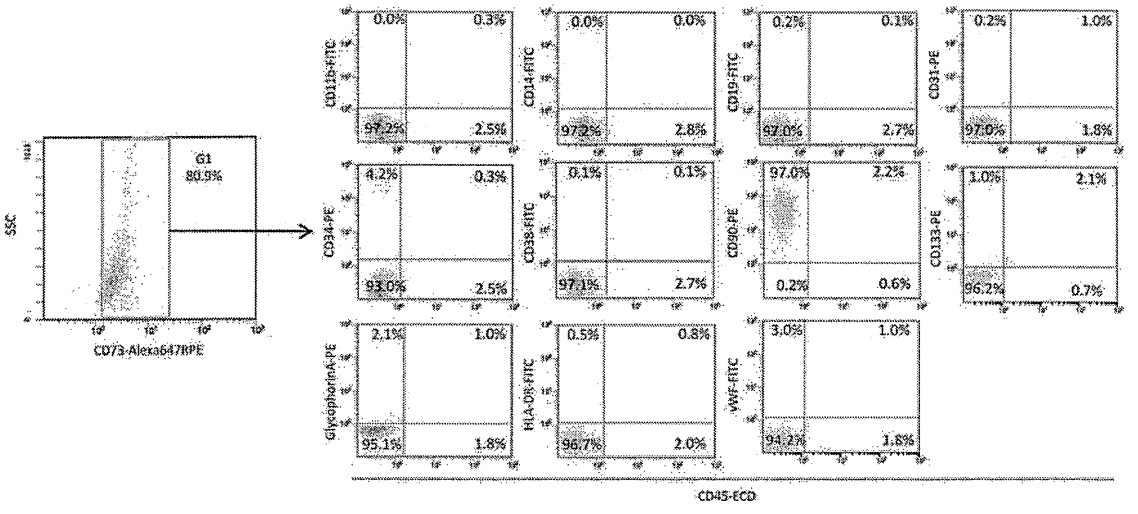

Figure 2. Multicolor analysis of freshly isolated MSC obtained by the modified protocol. To evaluate the presence of non-MSC, surface markers of freshly isolated cells were investigated. The majority of CD73-positive cells were negative for markers of hemocyte (CD11b, CD14, CD19, CD34, CD38, CD133, GlycophorinA, HLA-DR) and endothelial cell (CD31, vWF) lineages. It is notable that most of the CD73-positive cells expressed CD90, the latter not expressed on endothelial cells.

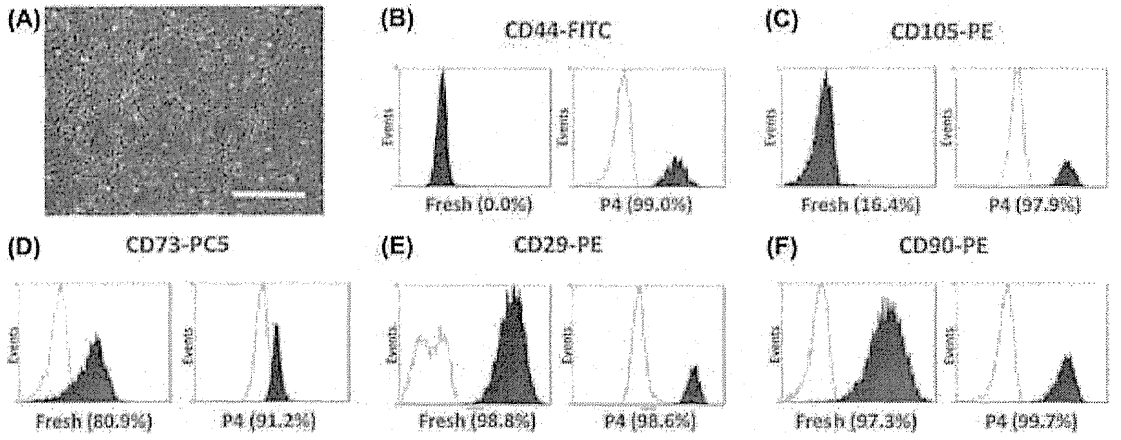

Figure 3. Changes in cell-surface markers associated with *in vitro* expansion. (A) Phase-contrast image of expanded UCMS cells. After *in vitro* expansion, analysis of MSC markers revealed an increased expression of CD44 (B), CD105 (C) and CD73 (D). In contrast, no change was observed in the expression of CD29 (E) and CD90 (F) because of *in vitro* expansion. Scale bar, 100 μm (A).

in multiple cell types including mesenchymal cells) and CD73 (Figure 3D; a nucleotidase expressed by multiple cells including mesenchymal cells) was increased in cells at passage 4. In contrast, expression of CD29 (Figure 3E; an integrin expressed in MSC) and CD90 (Figure 3F; a glycophosphatidylinositol-anchored cell-surface protein expressed by multiple cells including MSC) was similar to that observed prior to *ex vivo* expansion. These profiles were similar to amniotic-derived MSC as reported by De Coppi *et al.* (40).

Potential of UCMS cells

To investigate the potential of isolated UCMS cells to form differentiated cell types, the cell population was expanded under conditions conducive for osteocyte, chondrocyte or adipogenic differentiation. Under conditions conducive to the formation of osteocytes, on day 31 in cell culture Alizarin Red S-positive mineralized matrix-like nodules were observed (Figure 4A) and analysis of RNA confirmed the expression of osteocyte markers, osteopontin and alkaline phosphatase (ALP) (Figure 4B). Similarly, under conditions conducive to formation of a chondrogenic pellet, on day 21 in cell culture, Alcian Blue-positive chondrogenic-like pellets were observed (Figure 4C) and analysis of RNA confirmed the expression of chondrocyte markers, Sox-9 and aggrecan (Figure 4D). Under conditions leading to the formation of adipocytes, on day 20 of cell culture, Oil Red O-positive cells with lipid droplets were observed (Figure 4E, F) and analysis of RNA confirmed the expression of adipocyte marker peroxisome proliferator-activated receptor PPARγ2 (Figure 4G). Similarly, isolated cells incubated under conditions leading to neuronal differentiation showed subsequent expression of microtubule-associated protein 2 (MAP-2) and glial fibrillary acidic protein (GFAP) (Figure 4H). Furthermore, differentiated UCMS cells showed the myocyte marker MyoD (Figure 4I) and glucagon as a pancreatic cell marker (Figure 4J) when incubated under conditions leading to the formation of myocytes and pancreatic cells, respectively.

Suppression of GvHD by UCMS cells transplantation

In vitro-expanded MSC have been shown to suppress GvHD in patients after hematopoietic stem cell transplantation (41). To evaluate the potential for non-expanded UCMS cells to suppress GvHD, mice underwent allogeneic hematopoietic stem cell transplantation and were treated with non-expanded UCMS cells in RPMI. As a control, mice underwent allogeneic hematopoietic stem cell transplantation and were treated with RPMI alone. Mice were treated with non-expanded UCMS on days 0 and 6 after allogeneic stem cell transplantation, and the survival rate and severity of GvHD were investigated by 25 weeks after Bone Marrow Transplantation. (BMT). The frequency of severe GvHD at 6 weeks after allogeneic stem cell transplantation was significantly reduced with concomitant transplantation of non-expanded UCMS cells (Figure 4A). Although all mice in the control group showed severe GvHD or were already dead at 6 weeks, none of those treated with non-expanded UCMS cells (after the second treatment) were dead or showed severe GvHD. Representative pictures at 6 weeks in control and UCMS groups are shown in Figure 4B, C, respectively. Figure 4D shows the survival curve after allogeneic hematopoietic stem cell transplantation. Although no

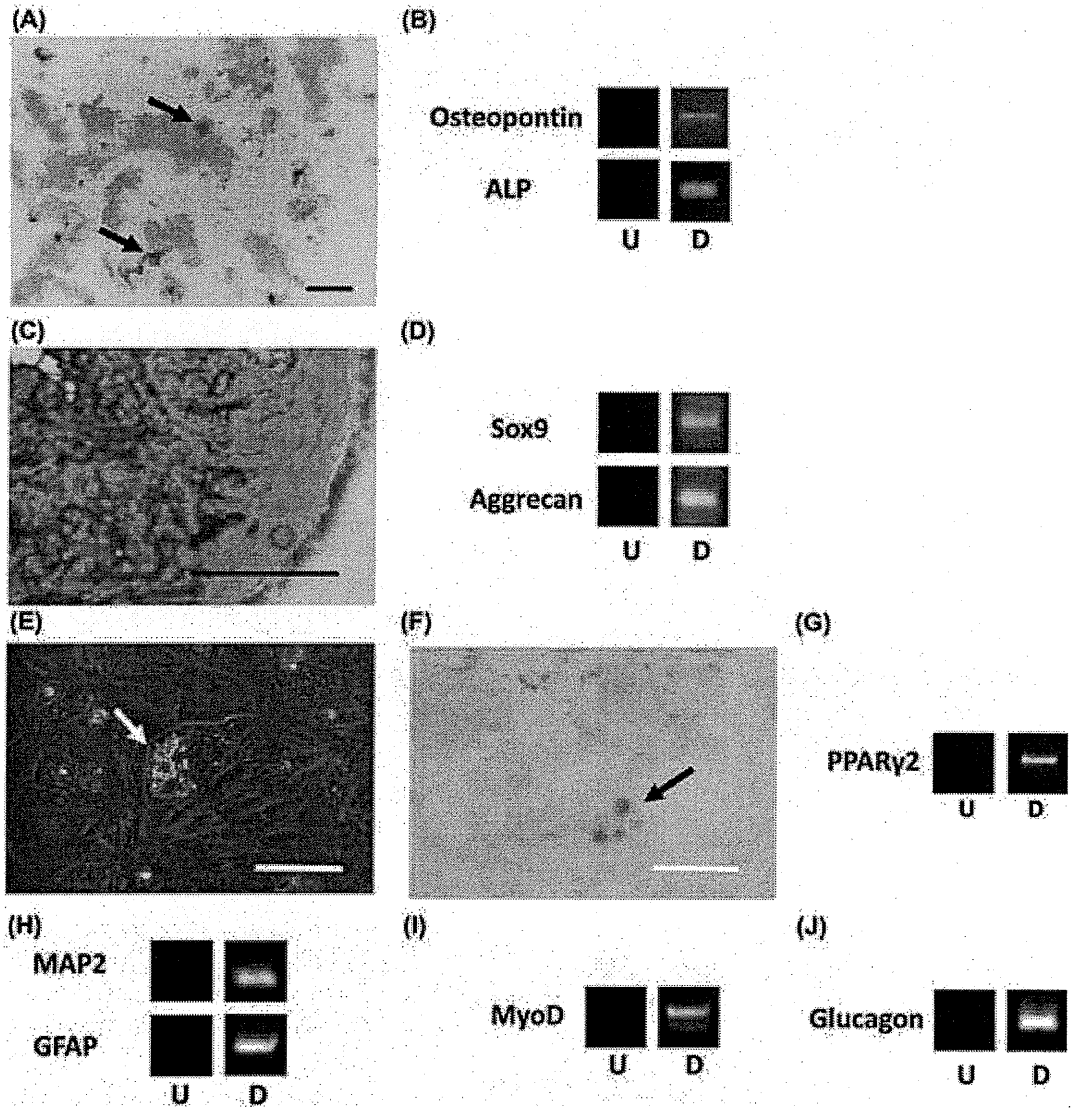

Figure 4. *In vitro* differentiation of freshly isolated UCMS cells. After expansion under conditions conducive to osteocyte or chondrocyte differentiation, Alizarin Red S-positive mineralized matrix-like nodules (A) or Alcian Blue-positive chondrogenic-like pellets (the latter displayed formation of layered structure at the surface) (C), respectively, were observed. UCMS cells cultured under conditions conductive to differentiation of osteocyte (B) and chondrocyte (D) cells expressed specific markers for each lineage. After expansion under conditions conducive to adipocyte differentiation, Oil Red O-positive adipocytes (E, phase-contrast image; F, Oil Red O staining) were observed and expression of PPARγ2 was observed (G). UCMS cells cultured under conditions conductive to differentiation of neuronal (H), myocyte (I) and pancreas (J) cells expressed specific markers for each lineage. Each experiment was repeated five times using different umbilical cord-derived cells. Scale bar, 40 μm (A), 100 μm (C, E, F). The arrow indicates Alizarin Red S-positive mineralized matrix-like nodules (A), lipid droplet (E) and Oil Red O-positive cells (F). U, undifferentiated; D, differentiated (B, D, G–J).

significant difference was apparent between groups at the 4-week assessment point, all of the mice in the control group were dead in 25 weeks, whereas no death was observed in mice with UCMS treatment group after the second treatment (Figure 5D).

Discussion

This study demonstrates that more than 2×10^7 MSC can be obtained safely from human umbilical cord without *in vitro* expansion and that these non-expanded MSC have the potential to suppress GvHD.

As a source of MSC, the umbilical cord has major advantages, including little contamination by cells of maternal origin, easy sterilization and few ethical problems. Compared with the method described by Weiss *et al.* (29), our modified method omits removal of blood vessels from the umbilical cord before treatment with collagenase and hyaluronidase.

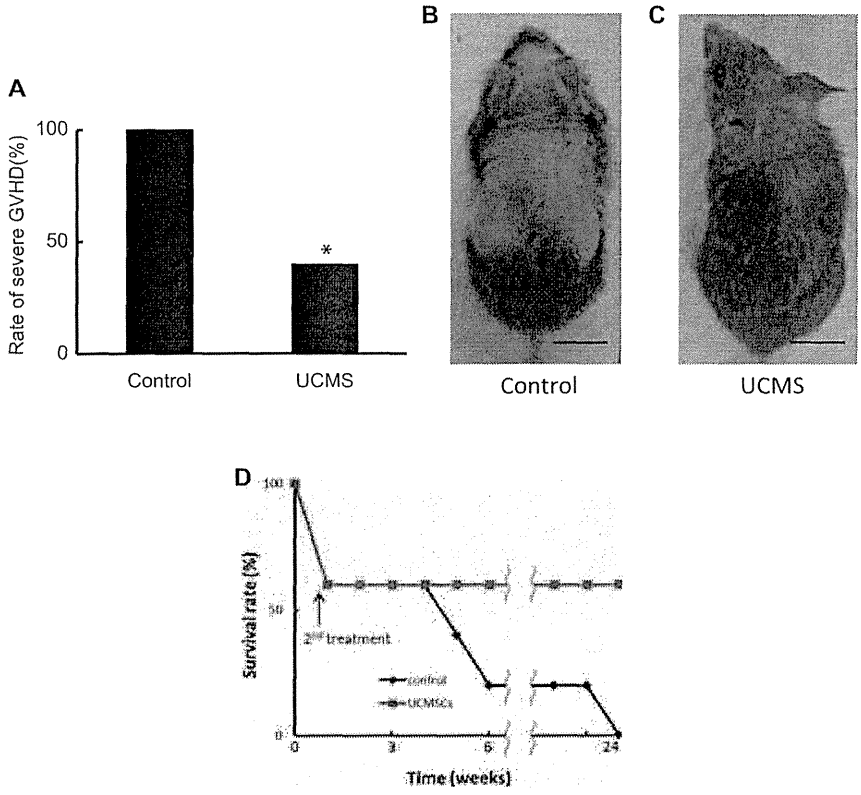

Figure 5. Suppression of GvHD by UCMS cells transplantation. Although all mice in the control group died or showed severe GvHD at 6 weeks (score 6; 1 mouse, dead; 4 mice), treatment with non-expanded UCMS cells significantly reduced the severity of GvHD (score 3; 1 mouse, score 4; 2 mice, dead; 2 mice) (A). Representative pictures of animals from the control group (B) and non-expanded UCMS cell-treated group (C) are shown. (D) Survival curve after radiation and allogeneic hematopoietic stem cell transplantation ($n = 5$, in each group). All of the mice in the control group were dead by 25 weeks after allogeneic hematopoietic stem cell transplantation. In contrast, no mice in the UCMS group were dead after the second infusion of non-expanded UCMS cells. $^*P < 0.05$ versus control. Scale bar, 1 cm (B, C).

Removal of the umbilical artery results in the loss of Wharton's jelly, which contains significant numbers of MSC. Preservation of the blood vessels before digestion with collagenase and hyaluronidase also significantly reduced contamination by endothelial cells. This finding may be attributed to removal of intact vascular structures from the cell suspension before digestion with trypsin, as vasculature was not considerably degraded in the presence of collagenase and hyaluronidase according to our protocol. Furthermore, our method has a significant advantage in that no *in vitro* cell culture is required for isolation of MSC from umbilical cord. In contrast, recently published methods described by Capelli *et al.* (11) and Lu *et al.* (10) involve cell culture over several days for isolation of MSC. The advantage of protocols using *in vitro* expansion is that non-adhesive cells can be removed, resulting in an enriched adhesive cell population. However, our results indicate that freshly isolated and non-selected umbilical cord-derived cells obtained by our method suppressed GvHD in an animal model. *In vitro* expansion of MSC carries a risk of tumorigenesis (42) and clinical use of the expanded cells requires strict monitoring to ensure safety. Our modified method has significant advantages in the reduced time required for the isolation procedure and its safety, both of which are important for cell banking. For the studies reported here, we used only the umbilical cords obtained at full-term Cesarean sections. It is likely that the properties and number of MSC in umbilical cord are similar comparing Cesarean section and vaginal delivery. Although caution should be taken regarding cleanliness/sterility after vaginal delivery, we expect that the same procedure can be used for umbilical cords obtained at full-term vaginal delivery.

In addition to offering a cell source for regenerative medicine, MSC have the potential to suppress GvHD after hematopoietic stem cell transplantation. Although the mechanisms and actual cell fraction underlying suppression of GvHD by MSC transplantation remains contentious (43), our results indicate

that human umbilical cord-derived non-expanded MSC suppressed GvHD in a murine model. The optimal type of MSC for suppression of GvHD, in terms of source, level of maturity and HLA-matching to the donor, is unclear. However, our results indicate that non-expanded UCMS cells represent a potential candidate cell source, particularly when co-banked with cord blood-derived hematopoietic cells (provided there is also strict control for contamination with infectious agents with HLA-typing). Furthermore, co-transplantation of HLA-matched hematopoietic stem cells and MSC may be advantageous to reduce clearance of transplanted MSC via immunologic recognition of HLA-matched hematopoietic cells.

In conclusion, our results indicate that umbilical cord-derived non-expanded MSC represent a potential cell source for cell banking and subsequent therapeutic use. Our results indicate that the combination of banking UCMS cells with identical cord blood-derived hematopoietic stem cells could be an important source for cell-based therapies in a range of settings.

Acknowledgments

This work was supported by a Grant-in-Aid for Scientific Research from the Ministry of Health, Labour and Welfare.

Declaration of interest: The authors declare no conflict of interest.

References

1. Liechty KW, MacKenzie TC, Shaaban AF, Radu A, Moseley AM, Deans R, et al. Human mesenchymal stem cells engraft and demonstrate site-specific differentiation after in utero transplantation in sheep. Nat Med. 2000;6:1282–6.
2. Schaffler A, Buchler C. Concise review. Adipose tissue-derived stromal cells: basic and clinical implications for novel cell-based therapies. Stem Cells. 2007;25:818–27.
3. Noth U, Osyczka AM, Tuli R, Hickok NJ, Danielson KG, Tuan RS. Multilineage mesenchymal differentiation potential of human trabecular bone-derived cells. J Orthop Res. 2002;20:1060–9.
4. De Bari C, Dell'Accio F, Luyten FP. Human periosteum-derived cells maintain phenotypic stability and chondrogenic potential throughout expansion regardless of donor age. Arthritis Rheum. 2001;44:85–95.
5. Hu Y, Liao L, Wang Q, Ma L, Ma G, Jiang X, et al. Isolation and identification of mesenchymal stem cells from human fetal pancreas. J Lab Clin Med. 2003;141:342–9.
6. in't Anker PS, Noort WA, Scherjon SA, Kleijburg-van der Keur C, Kruisselbrink AB, van Bezooijen RL, et al. Mesenchymal stem cells in human second-trimester bone marrow, liver, lung, and spleen exhibit a similar immunophenotype but a heterogeneous multilineage differentiation potential. Haematologica. 2003;88:845–52.
7. Huss R, Lange C, Weissinger EM, Kolb HJ, Thalmeier K. Evidence of peripheral blood-derived, plastic-adherent CD34(-/low) hematopoietic stem cell clones with mesenchymal stem cell characteristics. Stem Cells. 2000;18:252–60.
8. Rogers I, Casper RF. Umbilical cord blood stem cells. Best Pract Res Clin Obstet Gynaecol. 2004;18:893–908.
9. Romanov YA, Svintsitskaya VA, Smirnov VN. Searching for alternative sources of postnatal human mesenchymal stem cells: candidate MSC-like cells from umbilical cord. Stem Cells. 2003;21:105–10.
10. Lu LL, Liu YJ, Yang SG, Zhao QJ, Wang X, Gong W, et al. Isolation and characterization of human umbilical cord mesenchymal stem cells with hematopoiesis-supportive function and other potentials. Haematologica. 2006;91:1017–26.
11. Capelli C, Gotti E, Morigi M, Rota C, Weng L, Dazzi F, et al. Minimally manipulated whole human umbilical cord is a rich source of clinical-grade human mesenchymal stromal cells expanded in human platelet lysate. Cytotherapy. 2011;13:786–801.
12. Bjorklund A, Lindvall O. Cell replacement therapies for central nervous system disorders. Nat Neurosci. 2000;3:537–44.
13. Galle J, Bader A, Hepp P, Grill W, Fuchs B, Kas JA, et al. Mesenchymal stem cells in cartilage repair: state of the art and methods to monitor cell growth, differentiation and cartilage regeneration. Curr Med Chem. 2010;17:2274–91.
14. Liu H, Zhang J, Liu CY, Wang IJ, Sieber M, Chang J, et al. Cell therapy of congenital corneal diseases with umbilical mesenchymal stem cells: lumican null mice. PLoS One. 2010;5:1–4.
15. Lee JS, Hong JM, Moon GJ, Lee PH, Ahn YH, Bang OY. A long-term follow-up study of intravenous autologous mesenchymal stem cell transplantation in patients with ischemic stroke. Stem Cells. 2010;28:1099–106.
16. Schuleri KH, Feigenbaum GS, Centola M, Weiss ES, Zimmet JM, Turney J, et al. Autologous mesenchymal stem cells produce reverse remodelling in chronic ischaemic cardiomyopathy. Eur Heart J. 2009;30:2722–32.
17. Lim JH, Lee MH, Yi HG, Kim CS, Kim JH, Song SU. Mesenchymal stromal cells for steroid-refractory acute graft-versus-host disease: a report of two cases. Int J Hematol. 2010;92:204–7.
18. Portmann-Lanz CB, Schoeberlein A, Huber A, Sager R, Malek A, Holzgreve W, et al. Placental mesenchymal stem cells as potential autologous graft for pre- and perinatal neuroregeneration. Am J Obstet Gynecol. 2006;194:664–73.
19. in't Anker PS, Scherjon SA, Kleijburg-van der Keur C, Noort WA, Claas FH, Willemze R, et al. Amniotic fluid as a novel source of mesenchymal stem cells for therapeutic transplantation. Blood. 2003;102:1548–9.
20. Erices A, Conget P, Minguell JJ. Mesenchymal progenitor cells in human umbilical cord blood. Br J Haematol. 2000;109:235–42.
21. Wang HS, Hung SC, Peng ST, Huang CC, Wei HM, Guo YJ, et al. Mesenchymal stem cells in the Wharton's jelly of the human umbilical cord. Stem Cells. 2004;22:1330–7.
22. Meyer FA, Laver-Rudich Z, Tanenbaum R. Evidence for a mechanical coupling of glycoprotein microfibrils with collagen fibrils in Wharton's jelly. Biochim Biophys Acta. 1983;755:376–87.
23. McElreavey KD, Irvine AI, Ennis KT, McLean WH. Isolation, culture and characterisation of fibroblast-like cells derived from the Wharton's jelly portion of human umbilical cord. Biochem Soc Trans. 1991;19:29S.
24. Covas DT, Siufi JL, Silva AR, Orellana MD. Isolation and culture of umbilical vein mesenchymal stem cells. Braz J Med Biol Res. 2003;36:1179–83.

25. Sarugaser R, Lickorish D, Baksh D, Hosseini MM, Davies JE. Human umbilical cord perivascular (HUCPV) cells: a source of mesenchymal progenitors. Stem Cells. 2005;23:220–9.
26. Fu YS, Shih YT, Cheng YC, Min MY. Transformation of human umbilical mesenchymal cells into neurons in vitro. J Biomed Sci. 2004;11:652–60.
27. Fu YS, Cheng YC, Lin MY, Cheng H, Chu PM, Chou SC, et al. Conversion of human umbilical cord mesenchymal stem cells in Wharton's jelly to dopaminergic neurons in vitro: potential therapeutic application for Parkinsonism. Stem Cells. 2006;24:115–24.
28. Kadivar M, Khatami S, Mortazavi Y, Shokrgozar MA, Taghikhani M, Soleimani M. In vitro cardiomyogenic potential of human umbilical vein-derived mesenchymal stem cells. Biochem Biophys Res Commun. 2006;340:639–47.
29. Weiss ML, Medicetty S, Bledsoe AR, Rachakatla RS, Choi M, Merchav S, et al. Human umbilical cord matrix stem cells: preliminary characterization and effect of transplantation in a rodent model of Parkinson's disease. Stem Cells. 2006;24: 781–92.
30. Chao KC, Chao KF, Fu YS, Liu SH. Islet-like clusters derived from mesenchymal stem cells in Wharton's jelly of the human umbilical cord for transplantation to control type 1 diabetes. PLoS One. 2008;3:1–9.
31. Carlin R, Davis D, Weiss M, Schultz B, Troyer D. Expression of early transcription factors Oct-4, Sox-2 and Nanog by porcine umbilical cord (PUC) matrix cells. Reprod Biol Endocrinol. 2006;4:1–13.
32. Rubinstein P, Dobrila L, Rosenfield RE, Adamson JW, Migliaccio G, Migliaccio AR, et al. Processing and cryopreservation of placental/umbilical cord blood for unrelated bone marrow reconstitution. Proc Natl Acad Sci USA. 1995;92:10119–22.
33. Woodbury D, Reynolds K, Black IB. Adult bone marrow stromal stem cells express germline, ectodermal, endodermal, and mesodermal genes prior to neurogenesis. J Neurosci Res. 2002;69:908–17.
34. Dennis JE, Merriam A, Awadallah A, Yoo JU, Johnstone B, Caplan AI. A quadripotential mesenchymal progenitor cell isolated from the marrow of an adult mouse. J Bone Miner Res. 1999;14:700–9.
35. Reyes M, Lund T, Lenvik T, Aguiar D, Koodie L, Verfaillie CM. Purification and ex vivo expansion of postnatal human marrow mesodermal progenitor cells. Blood. 2001;98:2615–25.
36. Tang DQ, Cao LZ, Burkhardt BR, Xia CQ, Litherland SA, Atkinson MA, et al. In vivo and in vitro characterization of insulin-producing cells obtained from murine bone marrow. Diabetes. 2004;53:1721–32.
37. Taniguchi Y, Yoshihara S, Hoshida Y, Inoue T, Fujioka T, Ikegame K, et al. Recovery from established graft-vs-host disease achieved by bone marrow transplantation from a third-party allogeneic donor. Exp Hematol. 2008;36:1216–25.
38. Cooke KR, Kobzik L, Martin TR, Brewer J, Delmonte J Jr, Crawford JM, et al. An experimental model of idiopathic pneumonia syndrome after bone marrow transplantation. I. The roles of minor H antigens and endotoxin. Blood. 1996;88:3230–9.
39. Mutin M, Dignat-George F, Sampol J. Immunologic phenotype of cultured endothelial cells: quantitative analysis of cell surface molecules. Tissue Antigens. 1997;50:449–58
40. De Coppi P, Bartsch G Jr, Siddiqui MM, Xu T, Santos CC, Perin L, et al. Isolation of amniotic stem cell lines with potential for therapy. Nat Biotechnol. 2007;25:100–6.
41. Le Blanc K, Frassoni F, Ball L, Locatelli F, Roelofs H, Lewis I, et al. Mesenchymal stem cells for treatment of steroid-resistant, severe, acute graft-versus-host disease: a phase II study. Lancet. 2008;371:1579–86.
42. Spaeth EL, Dembinski JL, Sasser AK, Watson K, Klopp A, Hall B, et al. Mesenchymal stem cell transition to tumor-associated fibroblasts contributes to fibrovascular network expansion and tumor progression. PLoS One. 2009; 4:1–11.
43. Sato K, Ozaki K, Mori M, Muroi K, Ozawa K. Mesenchymal stromal cells for graft-versus-host disease : basic aspects and clinical outcomes. J Clin Exp Hematop. 2010;50:79–89.

STEM CELLS AND DEVELOPMENT
Volume 21, Number 13, 2012

DOI: 10.1089/scd.2011.0657

LETTER TO THE EDITOR

Leptomeningeal-Derived Doublecortin-Expressing Cells in Poststroke Brain

Takayuki Nakagomi,[1] Zoltán Molnár,[2] Akihiko Taguchi,[3] Akiko Nakano-Doi,[1] Shan Lu,[1,4] Yukiko Kasahara,[3] Nami Nakagomi,[5,6] and Tomohiro Matsuyama[1]

Increasing evidence indicates that neural stem/progenitor cells (NSPCs) reside in many regions of the central nervous system (CNS), including the subventricular zone (SVZ) of the lateral ventricle, subgranular zone of the hippocampal dentate gyrus, cortex, striatum, and spinal cord. Using a murine model of cortical infarction, we recently demonstrated that the leptomeninges (pia mater), which cover the entire cortex, also exhibit NSPC activity in response to ischemia. Pial-ischemia-induced NSPCs expressed NSPC markers such as nestin, formed neurosphere-like cell clusters with self-renewal activity, and differentiated into neurons, astrocytes, and oligodendrocytes, although they were not identical to previously reported NSPCs, such as SVZ astrocytes, ependymal cells, oligodendrocyte precursor cells, and reactive astrocytes. In this study, we showed that leptomeningeal cells in the poststroke brain express the immature neuronal marker doublecortin as well as nestin. We also showed that these cells can migrate into the poststroke cortex. Thus, the leptomeninges may participate in CNS repair in response to brain injury.

Introduction

USING A MURINE MODEL of cortical infarction [1], we recently demonstrated that the leptomeninges (pia mater), which cover the entire cortex, exhibit neural stem/progenitor cell (NSPC) activity in response to ischemia in adult brains [2]. Pial-ischemia-induced NSPCs (iNSPCs) expressed the NSPC marker nestin, formed neurosphere-like cell clusters with self-renewal ability, and differentiated into neurons, astrocytes, and oligodendrocytes [2], indicating that they have stem cell capacity similar to other NSPC types. However, we demonstrated that iNSPCs were not completely identical to previously described NSPCs [2], including subventricular zone astrocytes [3], ependymal cells [4], reactive astrocytes [5], resident glial cells [6], and oligodendrocyte precursor cells [7]. At almost the same time [2], Decimo et al. showed that spinal cord meninges were potential sources of stem/progenitor cells that undergo neuronal differentiation after injury [8]. These findings suggest that the leptomeninges that cover the entire central nervous system (CNS), including the brain [2] and spinal cord [8], may have a common repair system in response to injuries. To address this question, we labeled the pial cells using a green fluorescent protein (GFP) expression vector [1] and investigated their potential contribution to cortical neurogenesis in the poststroke brain.

Mice were sacrificed on day 3 after stroke and immunohistochemistry was performed [1,2,9,10]. Consistent with previous findings [2], cells in the poststroke leptomeninges expressed NSPC markers, such as nestin and vimentin (Fig. 1A–E). In an adherent monolayer culture [2,9], most pial cells isolated from the poststroke leptomeninges expressed nestin [2], while the number of nestin-positive cells coexpressing the immature neuronal cell marker doublecortin (DCX) increased under conditions conducive to differentiation [2,10] (Fig. 1F–H). DCX expression was also confirmed by reverse transcription–polymerase chain reaction (RT-PCR) (Fig. 1I) and western blot analysis (~45 kDa) (Fig. 1J). In the poststroke brain, DCX-positive cells were observed within the poststroke pia mater and cortex where they appeared to localize near nestin-positive cells (Fig. 2A); however, they were not observed in the nonischemic ipsilateral pia mater and cortex (Fig. 2B). To trace pial cells after brain injury, we labeled the leptomeninges in the left middle cerebral artery (MCA) area using a GFP-expressing vector 2 days before stroke (Fig. 2C, D). In the absence of ischemia, ~38.3% ± 12.5% GFP-positive leptomeningeal cells were observed in the MCA area and they were observed outside the laminin-positive cells [8], indicating that they were localized within the pia mater but not in cortical layer 1 (Fig. 2E). These GFP-positive cells did not express nestin and DCX at that time (data not shown), which

[1]Institute for Advanced Medical Sciences, Hyogo College of Medicine, Hyogo, Japan.
[2]Department of Physiology, Anatomy and Genetics, University of Oxford, Oxford, United Kingdom.
[3]Department of Regenerative Medicine Research, Institute of Biomedical Research and Innovation Hospital, Hyogo, Japan.
Departments of [4]Internal Medicine and [5]Pathology, Hyogo College of Medicine, Hyogo, Japan.
[6]Department of Pathology, Suita Municipal Hospital, Osaka, Japan.

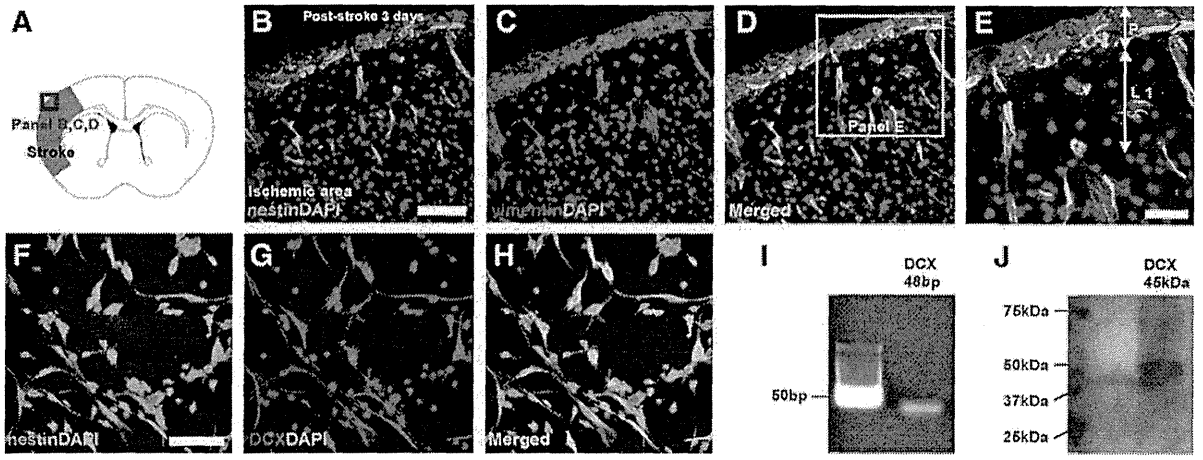

FIG. 1. Immunohistochemistry **(A)** showed that nestin- and vimentin-positive cells were present in the poststroke pia mater and cortex (nestin: **B, D, E,** green; vimentin: **C–E,** red; DAPI: **B–E,** blue). Three days after plating in the cell-differentiation-inducing medium, some of the nestin-positive cells isolated from the poststroke pia matter coexpressed DCX (nestin: **F, H,** green; DCX: **G, H,** red; DAPI: **F–H,** blue). DCX-positive cells were also confirmed by RT-PCR **(I)** and western blot **(J)** analyses. Scale bar: 100 μm **(B)** and 50 μm **(E** and **F)**. Results shown are representative of 5 replicates of the experimental protocol. DAPI, 4',6-diamino-2-phenylindole; DCX, doublecortin; L1, cortical layer 1; P, pia mater; RT-PCR, reverse transcription–polymerase chain reaction.

agreed with reports that nestin- [2] and DCX-positive cells (Fig. 2B) are not found in the leptomeninges in the absence of ischemia. However, some GFP-labeled pial cells within the poststroke area coexpressed nestin (Fig. 2F) and DCX (Fig. 2G) on day 3 after stroke, and they migrated to the poststroke cortex (Fig. 2F, G). Although GFP-positive cells were also observed in the nonischemic ipsilateral leptomeninges (<10%) on day 3 after stroke, they did not express nestin and DCX (data not shown), which agreed with a study that observed nestin-positive cells in the ischemic pia mater but not nonischemic pia mater [2]. These results indicate that in response to ischemia, pial cells generate nestin-positive cells that were presumably iNSPCs [2] and DCX-positive immature neurons in the poststroke cortex, indicating their potential contribution to cortical regeneration. However, the number of DCX-positive cells in the poststroke pia mater and cortex gradually decreased at subsequent time points (Fig. 2H), which was consistent with the number of nestin-positive iNSPCs [2]. Thus, to further investigate the potential contribution of leptomeningeal cells to cortical neurogenesis in the poststroke brain, we obtained brain slices 3 days after stroke and incubated them for 7 days in a medium containing basic fibroblast growth factor (bFGF) and epidermal growth factor (EGF), as described previously [2], which promoted the proliferation of pial iNSPCs. DCX-positive cells were not observed in the nonischemic ipsilateral pia mater and cortex (Fig. 2I), but numerous cells were observed in the poststroke pia mater and cortex (Fig. 2J) together with an increased number of nestin-positive cells (Fig. 2K–M).

In the present study, we found that DCX-positive cells were developed in the poststroke pia mater and cortex as well as nestin-positive cells [2], although they were not observed in the nonischemic ipsilateral pia mater and cortex. These findings suggest that ischemia is essential for the induction of NSPCs and/or neuronal progenitors in these regions. In developing embryos, DCX was initially expressed in the outer cortical region preplate, which is covered by pia during the early stages, and this expression pattern extended into the intermediate zone during the later stages [11]. As with the developmental findings, DCX-positive immature neurons were also observed in response to ischemia, predominantly in the cortical surface adjacent to the injured regions, that is, the poststroke pia mater rather than the poststroke cortex. We also demonstrated in vivo generation of DCX-positive newborn neurons in the poststroke pia mater and cortex from the early poststroke period. These findings were consistent with a previous report that demonstrated cortical neurogenesis from the acute phases after ischemia in vivo [12]. Although the cells isolated from the poststroke pia mater could differentiate into mature neurons expressing microtubule-associated protein 2 (MAP2) in vitro [2], the DCX-positive immature neurons developing in the poststroke pia mater and cortex decreased at later time points (Fig. 2H) and no MAP2-positive mature neurons were present in these regions until 60 days after stroke in vivo (data not shown). These findings were consistent with our previous study, which showed that mature neurons from iNSPCs could be observed only in the peristroke cortex [9,10] and not in the poststroke cortex [1]. Overall, these results may suggest that local factors present in the in vivo poststroke milieu [13,14] prevent newborn neurons from surviving for a long period; hence, they cannot differentiate into mature neurons. It would be challenging to accomplish cortical neurogenesis within the poststroke cortex after permanent ischemia in vivo; however, an abundance of DCX-positive immature neurons could develop in the poststroke pia mater and cortex if poststroke brains were incubated in a medium containing growth factors. These results suggest that cortical neurogenesis within the poststroke area may become a reality in future via the control of multiple factors.

Although the precise source, lineage, and traits of leptomeningeal progenitors, including DCX- and nestin-positive

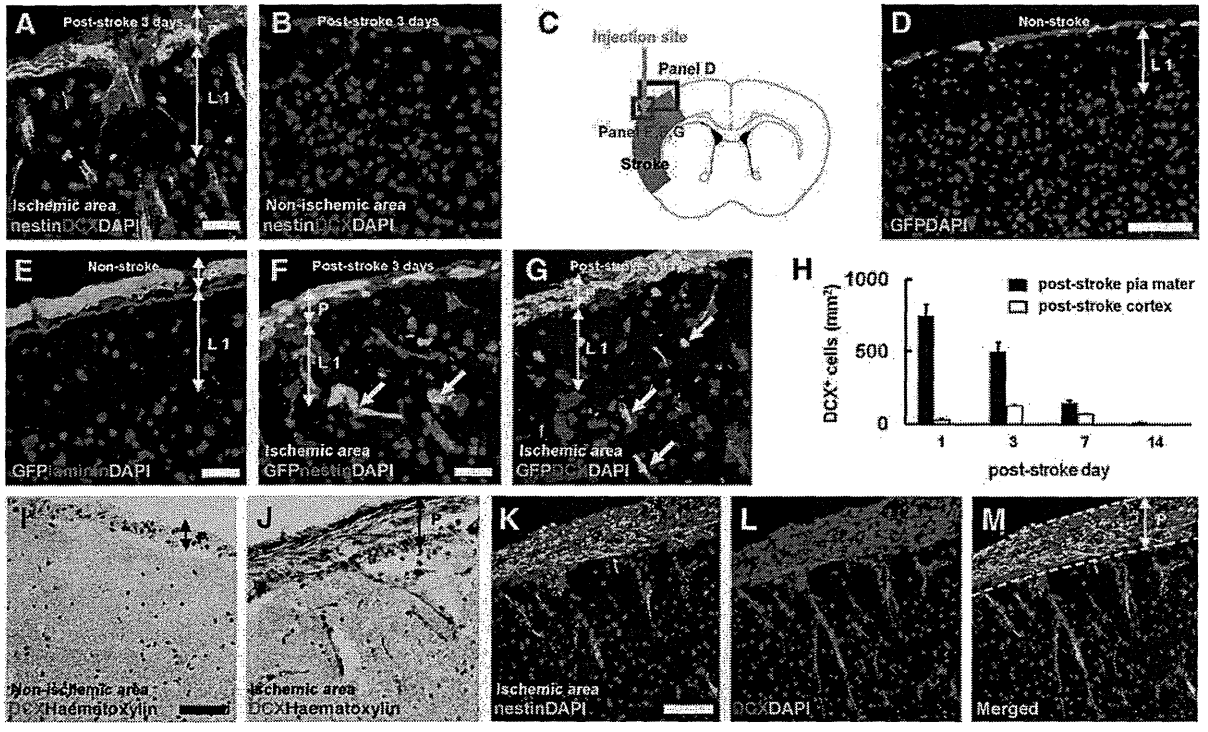

FIG. 2. DCX-positive cells were observed near nestin-positive cells in the poststroke pia mater and cortex (DCX: **A,** *red;* nestin: **A,** *green;* DAPI: **A,** *blue*), although they were not observed in the nonischemic ipsilateral pia mater and cortex (DCX: **B,** *red;* nestin: **B,** *green;* DAPI: **B,** *blue*). Some pial cells, which were labeled with a GFP-expressing vector (**C,** GFP: **D, E,** *green;* laminin: **E,** *red;* DAPI: **D, E,** *blue*), migrated into the poststroke cortex after ischemia where they expressed nestin (*arrows*) (GFP: **F,** *green;* nestin: **F,** *red;* DAPI: **F,** *blue*) and DCX (*arrows*) (GFP: **G,** *green;* DCX: **G,** *red;* DAPI: **G,** *blue*). However, the number of DCX-positive cells in the poststroke pia mater and cortex decreased gradually at later time points (**H**). To investigate the potential contribution of leptomeningeal cells to cortical repair, brain slices were incubated in a medium that accelerated the proliferation of pial iNSPCs. Although DCX immunohistochemistry using the DAB reaction showed that DCX-positive cells were not observed in the nonischemic ipsilateral pia mater and cortex (**I**), it was confirmed that DCX-positive cells could survive and proliferate in the poststroke pia mater and cortex (**J**) as well as in the expanding nestin-positive cells (nestin: **K, M,** *green;* DCX: **L, M,** *red;* DAPI: **K–M,** *blue*). Scale bar: 100 μm (**D, I,** and **K**) and 50 μm (**A, E,** and **F**). Results shown are representative of 5 replicates of the experimental protocol. DAB, diaminobenzidine; GFP, green fluorescent protein; iNSPCs, ischemia-induced neural stem/progenitor cells.

cells, remain unclear, we showed that pial iNSPCs may originate partially from the neural crest–pericyte lineage [2], suggesting that they are indeed a novel NSPC population. Experimental lineage labeling of the leptomeninges, pericytes, and/or neural crests by genetic means may help clarify the precise characteristics of leptomeningeal cells in the poststroke brain in future studies. Accumulating evidence in the field of cardiology has also shown that cardiac stem/progenitor cells residing in the epicardium, known as epicardial progenitor cells, are activated in the adult heart after injury and that they give rise to de novo cardiomyocytes [15,16]. These findings may indicate that stem/progenitor cells are present on the surfaces of multiple organs, in addition to those observed in the CNS [2,8,17] and heart [15,16]. There are additional issues and questions to be addressed. However, the results of recent studies on leptomeninges-associated NSPCs [2,8,17] and the present study support the hypothesis that the leptomeninges that cover the entire CNS, including the brain [2] and spinal cord [8], may give rise to immature neuronal cells with an important role in CNS restoration. Thus, the leptomeninges may become a new target for treatment of various CNS diseases, including brain and spinal cord injuries.

Materials and Methods

Induction of focal cerebral ischemia

All procedures were approved by the Animal Care Committee of Hyogo College of Medicine. Six-week-old male CB-17/Icr-+/+Jcl mice (Clea Japan, Inc.) were subjected to cerebral ischemia. Permanent focal cerebral ischemia was induced by ligation of the distal portion of the left MCA [1,2,9,10,13,18]. In brief, the left MCA was isolated, electrocauterized, and disconnected immediately distal to the point where it crossed the olfactory tract (distal M1 portion), under halothane inhalation. The infarct area in mice with this background is known to be highly reproducible and limited to the ipsilateral cerebral cortex [1,2,9,10,13,18]. Quantitative analyses were performed by investigators who were blinded to the experimental protocol and the identities of the study samples.

Histological analysis

Immunohistochemistry was performed as described previously [1,2,9,10]. In brief, mice were deeply anesthetized with sodium pentobarbital (50 mg/kg) and perfused transcardially with 4% paraformaldehyde. Coronal brain sections (20 μm) were prepared and stained with antibodies to nestin (Chemicon), vimentin (Santa Cruz Biotechnology), laminin (Sigma), MAP2 (Chemicon), and DCX (LifeSpan Biosciences). Primary antibodies were visualized using Alexa Fluor 488- or 555-conjugated secondary antibodies (Molecular probes). Nuclei were stained with 4′,6-diamino-2-phenylindole (DAPI) (Kirkegaard & Perry Laboratories). Images of sections were captured using a confocal laser microscope (LSM510; Carl Zeiss). The poststroke pia mater or cortex was measured (total of 50 data points/group, ie, 10 sections/mouse, $n=5$) using Image J software downloaded from NIH Image, and the number of DCX-positive cells was counted as described previously [1,2,10,13]. Results were reported as the mean ± standard deviation. To trace the leptomeningeal cells after ischemia, the mice were anesthetized and placed in a stereotactic apparatus, before a lentiviral vector encoding GFP [5.2×10^5 transducing unit (TU)/μL] [19] was injected into the pia mater of the MCA area (0.3 μL, at 2.5-mm lateral and 1.5-mm rostral from the bregma) as described previously [1,2,9]. To evaluate the efficiency of GFP transduction in leptomeninges, coronal sections (20 μm) located ± 200 μm anterior–posterior from the injection site were prepared and the ratio of GFP-positive cells to leptomenigeal cells was quantified in the poststroke pia mater. In another set of experiments, whole brains were removed after ischemia and coronal brain slices (6-mm thick) were incubated in Dulbecco's modified Eagle's medium (Invitrogen) containing 20 ng/mL of bFGF (Peprotech) and 20 ng/mL of EGF (Peprotech). Brain sections were then fixed, cut into 20-μm-thick sections with a cryostat, and subjected to immunohistochemistry [2].

Reverse transcription–polymerase chain reaction

Total RNA was extracted from the poststroke pia mater, and cDNA was amplified under the following conditions [2]: 15 s at 94°C, 30 s at 56°C, and 1 min at 68°C (40 cycles). The primer sequences were as follows: DCX forward: AGAGGG TCACGGATGAATGGA and DCX reverse: GTGGGCACTA TGAGTGGGAC (amplicon size, 48 bp).

Western blot analysis

Pial cells were isolated from the poststroke leptomeninges at 3 days after stroke. Next, they were incubated in medium containing bFGF and EGF in an adherent monolayer culture [2,9], followed by incubation under differentiating conditions [2,10]. The cells were collected after trypsin treatment and samples were separated by 10% sodium dodecyl sulfate–polyacrylamide gel electrophoresis. Separated proteins (10 μg) were transferred electrophoretically onto nitrocellulose membranes. The membranes were incubated with anti-DCX antibody (LifeSpan Biosciences) and peroxidase-labeled secondary antibodies. Antibody labeling of protein bands was detected using enhanced chemiluminescence reagents (Chemi-Lumi One; Nacalai Tesque) according to the manufacturer's instructions.

Acknowledgments

This work was partially supported by a Grant-in-Aid for scientific research from the Ministry of Education, Culture, Sports, Science and Technology (21700363), Takeda Science Foundation (2009), and Grant-in-Aid for researchers, Hyogo College of Medicine (2011). We would like to thank Ms. Y. Okinaka and Dr. S. Kubo for technical assistance.

Author Disclosure Statement

The authors have declared that no conflict of interest exists.

References

1. Nakagomi T, A Taguchi, Y Fujimori, O Saino, A Nakano-Doi, S Kubo, A Gotoh, T Soma, H Yoshikawa, et al. (2009). Isolation and characterization of neural stem/progenitor cells from post-stroke cerebral cortex in mice. Eur J Neurosci 29:1842–1852.
2. Nakagomi T, Z Molnar, A Nakano-Doi, A Taguchi, O Saino, S Kubo, M Clausen, H Yoshikawa, N Nakagomi and T Matsuyama. (2011). Ischemia-induced neural stem/progenitor cells in the pia mater following cortical infarction. Stem Cells Dev 20:2037–2051.
3. Doetsch F, I Caille, DA Lim, JM Garcia-Verdugo and A Alvarez-Buylla. (1999). Subventricular zone astrocytes are neural stem cells in the adult mammalian brain. Cell 97: 703–716.
4. Moreno-Manzano V, FJ Rodriguez-Jimenez, M Garcia-Rosello, S Lainez, S Erceg, MT Calvo, M Ronaghi, M Lloret, R Planells-Cases, JM Sanchez-Puelles and M Stojkovic. (2009). Activated spinal cord ependymal stem cells rescue neurological function. Stem Cells 27:733–743.
5. Shimada IS, BM Peterson and JL Spees. (2010). Isolation of locally derived stem/progenitor cells from the peri-infarct area that do not migrate from the lateral ventricle after cortical stroke. Stroke 41:e552–e560.
6. Zawadzka M, LE Rivers, SP Fancy, C Zhao, R Tripathi, F Jamen, K Young, A Goncharevich, H Pohl, et al. (2010). CNS-resident glial progenitor/stem cells produce Schwann cells as well as oligodendrocytes during repair of CNS demyelination. Cell Stem Cell 6:578–590.
7. Kondo T and M Raff. (2000). Oligodendrocyte precursor cells reprogrammed to become multipotential CNS stem cells. Science 289:1754–1757.
8. Decimo I, F Bifari, FJ Rodriguez, G Malpeli, S Dolci, V Lavarini, S Pretto, S Vasquez, M Sciancalepore, et al. (2011). Nestin- and doublecortin-positive cells reside in adult spinal cord meninges and participate in injury-induced parenchymal reaction. Stem Cells 29:2062–2076.
9. Nakagomi N, T Nakagomi, S Kubo, A Nakano-Doi, O Saino, M Takata, H Yoshikawa, DM Stern, T Matsuyama and A Taguchi. (2009). Endothelial cells support survival, proliferation, and neuronal differentiation of transplanted adult ischemia-induced neural stem/progenitor cells after cerebral infarction. Stem Cells 27:2185–2195.
10. Nakano-Doi A, T Nakagomi, M Fujikawa, N Nakagomi, S Kubo, S Lu, H Yoshikawa, T Soma, A Taguchi and T Matsuyama. (2010). Bone marrow mononuclear cells promote proliferation of endogenous neural stem cells through vascular niches after cerebral infarction. Stem Cells 28:1292–1302.

11. Boekhoorn K, A Sarabdjitsingh, H Kommerie, K de Punder, T Schouten, PJ Lucassen and E Vreugdenhil. (2008). Doublecortin (DCX) and doublecortin-like (DCL) are differentially expressed in the early but not late stages of murine neocortical development. J Comp Neurol 507:1639–1652.
12. Ohira K, T Furuta, H Hioki, KC Nakamura, E Kuramoto, Y Tanaka, N Funatsu, K Shimizu, T Oishi, et al. (2010). Ischemia-induced neurogenesis of neocortical layer 1 progenitor cells. Nat Neurosci 13:173–179.
13. Saino O, A Taguchi, T Nakagomi, A Nakano-Doi, S Kashiwamura, N Doe, N Nakagomi, T Soma, H Yoshikawa, et al. (2010). Immunodeficiency reduces neural stem/progenitor cell apoptosis and enhances neurogenesis in the cerebral cortex after stroke. J Neurosci Res 88:2385–2397.
14. Takata M, T Nakagomi, S Kashiwamura, A Nakano-Doi, O Saino, N Nakagomi, H Okamura, O Mimura, A Taguchi and T Matsuyama. (2011). Glucocorticoid-induced TNF receptor-triggered T cells are key modulators for survival/death of neural stem/progenitor cells induced by ischemic stroke. Cell Death Differ [Epub ahead of print]; DOI: 10.1038/cdd.2011.145.
15. Zhou B, Q Ma, S Rajagopal, SM Wu, I Domian, J Rivera-Feliciano, D Jiang, A von Gise, S Ikeda, KR Chien and WT Pu. (2008). Epicardial progenitors contribute to the cardiomyocyte lineage in the developing heart. Nature 454: 109–113.
16. Smart N, S Bollini, KN Dube, JM Vieira, B Zhou, S Davidson, D Yellon, J Riegler, AN Price, MF Lythgoe, WT Pu and PR Riley. (2011). *De novo* cardiomyocytes from within the activated adult heart after injury. Nature 474:640–644.
17. Bifari F, I Decimo, C Chiamulera, E Bersan, G Malpeli, J Johansson, V Lisi, B Bonetti, G Fumagalli, G Pizzolo and M Krampera. (2009). Novel stem/progenitor cells with neuronal differentiation potential reside in the leptomeningeal niche. J Cell Mol Med 13:3195–3208.
18. Taguchi A, T Soma, H Tanaka, T Kanda, H Nishimura, H Yoshikawa, Y Tsukamoto, H Iso, Y Fujimori, et al. (2004). Administration of CD34+ cells after stroke enhances neurogenesis via angiogenesis in a mouse model. J Clin Invest 114:330–338.
19. Kubo S, MC Seleme, HS Soifer, JL Perez, JV Moran, HH Kazazian Jr. and N Kasahara. (2006). L1 retrotransposition in nondividing and primary human somatic cells. Proc Natl Acad Sci U S A 103:8036–8041.

Address correspondence to:
Dr. Takayuki Nakagomi
Institute for Advanced Medical Sciences
Hyogo College of Medicine
1-1 Mukogawacho, Nishinomiya
Hyogo 663-8501
Japan

E-mail: nakagomi@hyo-med.ac.jp

Received for publication November 24, 2011
Accepted after revision February 17, 2012
Prepublished on Liebert Instant Online February 18, 2012

Cell Death and Differentiation (2012) 19, 756–767

www.nature.com/cdd

Open

Glucocorticoid-induced TNF receptor-triggered T cells are key modulators for survival/death of neural stem/progenitor cells induced by ischemic stroke

M Takata[1,3,5], T Nakagomi[1,5], S Kashiwamura[2,5], A Nakano-Doi[1], O Saino[1], N Nakagomi[1], H Okamura[2], O Mimura[3], A Taguchi[4] and T Matsuyama*[,1]

Increasing evidences show that immune response affects the reparative mechanisms in injured brain. Recently, we have demonstrated that CD4$^+$T cells serve as negative modulators in neurogenesis after stroke, but the mechanistic detail remains unclear. Glucocorticoid-induced tumor necrosis factor (TNF) receptor (GITR), a multifaceted regulator of immunity belonging to the TNF receptor superfamily, is expressed on activated CD4$^+$T cells. Herein, we show, by using a murine model of cortical infarction, that GITR triggering on CD4$^+$T cells increases poststroke inflammation and decreases the number of neural stem/progenitor cells induced by ischemia (iNSPCs). CD4$^+$GITR$^+$T cells were preferentially accumulated at the postischemic cortex, and mice treated with GITR-stimulating antibody augmented poststroke inflammatory responses with enhanced apoptosis of iNSPCs. In contrast, blocking the GITR–GITR ligand (GITRL) interaction by GITR–Fc fusion protein abrogated inflammation and suppressed apoptosis of iNSPCs. Moreover, GITR-stimulated T cells caused apoptosis of the iNSPCs, and administration of GITR-stimulated T cells to poststroke severe combined immunodeficient mice significantly reduced iNSPC number compared with that of non-stimulated T cells. These observations indicate that among the CD4$^+$T cells, GITR$^+$CD4$^+$T cells are major deteriorating modulators of poststroke neurogenesis. This suggests that blockade of the GITR–GITRL interaction may be a novel immune-based therapy in stroke.
Cell Death and Differentiation (2012) **19,** 756–767; doi:10.1038/cdd.2011.145; published online 4 November 2011

Brain injury induces acute inflammation, thereby exacerbating poststroke neuronal damage.[1–4] Although central nervous system (CNS) is known for its limited reparative capacity, inflammation is a strong stimulus for reparative mechanisms including activation of neurogenesis. However, the latter results in low survival of newly generated neural stem cells.[5] These findings indicate the relevance of endogenous regulatory and/or environmental factors for survival and differentiation of neural stem cells.

In a murine model of cerebral ischemia, we have detected neural stem/progenitor cells induced by ischemia (ischemia-induced neural stem/progenitor cells; iNSPCs) in the poststroke cerebral cortex.[6] More recently, we have observed spontaneous accelerated repair in severe combined immunodeficient mice (SCID) compared with immunocompetent wild-type controls,[7] and have demonstrated that CD4$^+$T cells serve as negative regulators in the survival of iNSPCs.[8] Together with previous reports supporting the importance of the role of T cells in regulating poststroke inflammation[1,2,9] and functional recovery,[1,10,11] these findings emphasize on the link between CD4$^+$T cells and survival of iNSPCs. However, the mechanistic details and the subpopulation of CD4$^+$T cells responsible for acting as negative regulators in CNS repair remain unclear.

Glucocorticoid-induced tumor necrosis factor (TNF) receptor (GITR)-related protein that was originally cloned in a glucocorticoid-treated hybridoma T-cell line[12] is a protein belonging to the TNF receptor superfamily. It is expressed at basal levels in responder resting T cells, with CD4$^+$T cells including CD4$^+$CD25$^+$T cells (regulatory T cell, Treg) having a higher GITR expression than CD8$^+$T cells.[13] When the T cells are activated, GITR is strongly upregulated in responder CD4$^+$T cells. In this situation, the stimulatory effect of responder T cells was more activated[13,14] and the suppressing effect of Treg was completely abrogated,[13] leading to a more enhanced immune/inflammatory response.[15] In the CNS, it has been reported that blocking of the GITR–GITR ligand (GITRL) interaction protected spinal cord injury from

[1]Laboratory of Neurogenesis and CNS Repair, Hyogo College of Medicine, 1-1 Mukogawacho, Nishinomiya, Hyogo 663-8501, Japan; [2]Laboratory of Self Defense, Institute for Advanced Medical Sciences, Hyogo College of Medicine, 1-1 Mukogawacho, Nishinomiya, Hyogo 663-8501, Japan; [3]Department of Ophthalmology, Hyogo College of Medicine, 1-1 Mukogawacho, Nishinomiya, Hyogo 663-8501, Japan and [4]Department of Cerebrovascular Disease, National Cardiovascular Research Center, Osaka 565-8565, Japan
*Corresponding author: T Matsuyama, Laboratory of Neurogenesis and CNS Repair, Institute for Advanced Medical Sciences, Hyogo College of Medicine, 1-1 Mukogawacho, Nishinomiya, Hyogo 663-8501, Japan. Tel: +81 798 45 6821; Fax: +81 798 45 6823; E-mail: tomohiro@hyo-med.ac.jp
[5]These authors contributed equally to this work.
Keywords: GITR; Fas; T-cell; neural stem cell; ischemia
Abbreviations: BrdU, 5-bromo-2′-deoxyuridine; CNS, central nervous system; DAPI, 4′,6-diamino-2-phenylindole; EGF, epidermal growth factor; FasL, Fas ligand; GAPDH, glyceraldehyde-3-phosphate dehydrogenase; GITR, glucocorticoid-induced tumor necrosis factor receptor; GITRL, GITR ligand; GFP, green fluorescent protein; gld, generalized lymphoproliferative disorder = spontaneous mutation in the Fas ligand gene; iNSPC, ischemia-induced neural stem/progenitor cell; MCA, middle cerebral artery; SCID, severe combined immunodeficient; Sox2, SRY (sex determining region Y)-box 2; TCR, T-cell receptor; Treg, regulatory T cell
Received 23.5.11; revised 06.9.11; accepted 27.9.11; Edited by JA Cidlowski; published online 04.11.11

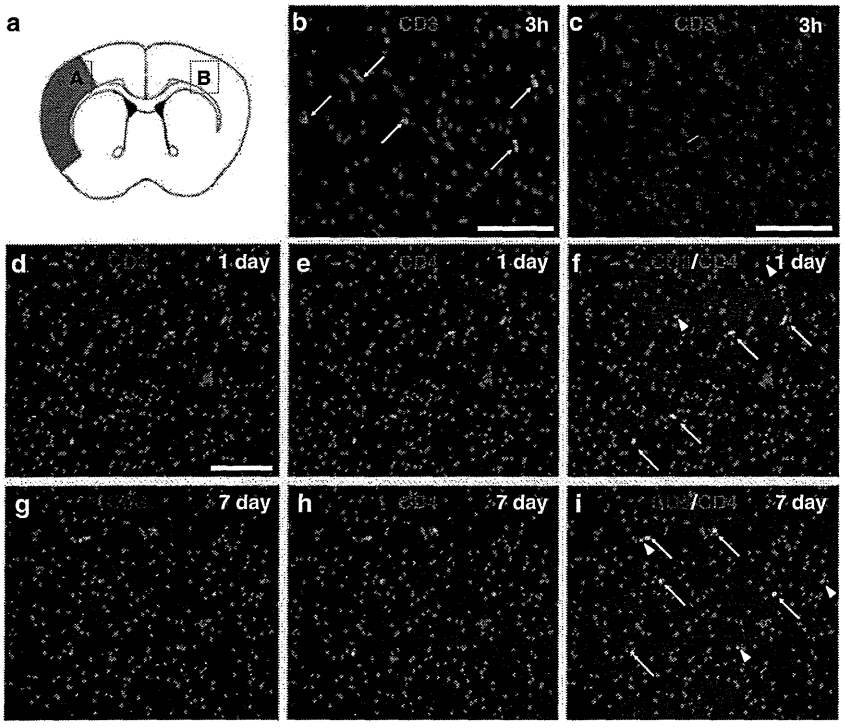

Figure 1 T-cell infiltration into the ischemic area of the poststroke brain. Immunohistochemistry for $CD3^+$ cells (T cells; (**a**) B: ischemic area and C: contralateral cortex) and $CD4^+$T cells (**d–i**) infiltrated into the postischemic cortex 3 h (**b** and **c**), 1 day (**d**) and 7 days (**g**) after stroke. $CD3^+$ T cells were positive for CD4 1 day and 7 days (arrows, **d** and **g**: CD3; **e** and **h**: CD4; **f** and **i**: merged, nuclei were counterstained with DAPI) after stroke. Arrowheads indicate $CD4^-$ T cells (**f** and **i**). (**b–i**) Scale bar: 100 μm

the inflammatory response,[16] whereas GITR triggering worsened experimental autoimmune encephalomyelitis while stimulating autoreactive $CD4^+$T cells.[17] These observations lead us to hypothesize that GITR triggering on T cells may serve as a negative regulator for CNS repair after cerebral infarction.

In this study, we demonstrated for the first time that GITR triggering on T cells following ischemic stroke enhanced poststroke inflammation and cell death of iNSPCs. Administration of GITR–Fc fusion protein markedly suppressed these responses. In addition, GITR-triggered T cells directly induced apoptosis of iNSPCs *in vitro*. Our current results show that activated $GITR^+$T cells acted as negative modulators for CNS restoration, indicating that blockade of the GITR–GITRL interaction can be a novel strategy for treating ischemic stroke.

Results

Infiltration of $CD4^+GITR^+$T cells into the ischemic cortex after stroke. Immunohistochemistry (Figures 1a–c) revealed that $CD3^+$ cells (T cells) appeared to infiltrate the ischemic region as early as 3 h after stroke (Figure 1b) and were observed continuously during the poststroke period (Figures 1d and g). The T cells were rarely observed at nonischemic ipsilateral or contralateral cortex (Figure 1c). Most T cells in the ischemic region (~70% of T cells) were CD4 positive (Figures 1d–i), indicating that $CD4^+$T cells predominantly infiltrate the poststroke cortex. However, GITR-positive cells were not found in the ischemic region at 6 h after stroke (Figure 2a), whereas a number of T cells were detected at the same region (Figures 2b and c). This indicates that GITR was not expressed in the infiltrated T cells at early poststroke period. GITR-expressing cells started to appear at 24 h after stroke and gradually increased in number. At 7 days post stroke, a number of $CD3^+$T cells co-express GITR (Figures 2d–f). Calculating the number of infiltrated T cells in serial brain sections revealed that ~65% of $CD4^+$T cells were GITR positive, indicating that $GITR^+$ T cells predominantly occupied the subset of $CD4^+$T cells at the late poststroke period. Semiquantitative analysis for the number of $CD4^+$T or $GITR^+$ cells in the ischemic region is shown in Figure 2g.

Predominant accumulation of $CD4^+GITR^+$T cells at the ischemic cortex after stroke. To confirm the enhanced expression of GITR on $CD4^+$T cells, we assessed the subset of T cells by FACS analysis using the cells extracted from the ischemic cortex[18] (Figures 3a and b). Consistent with the previous report, the brain extract contained substantial amount of mononuclear cells (Figure 3b) and FACS analysis detected a distinct subset of lymphocytes that had infiltrated the ischemic cortex (Figures 3c–f). We detected about 20% $CD4^+$T cells extracted from the infarcted brain tissue. We at first gated $CD3^+$ cells and then analyzed CD25 to characterize the corresponding

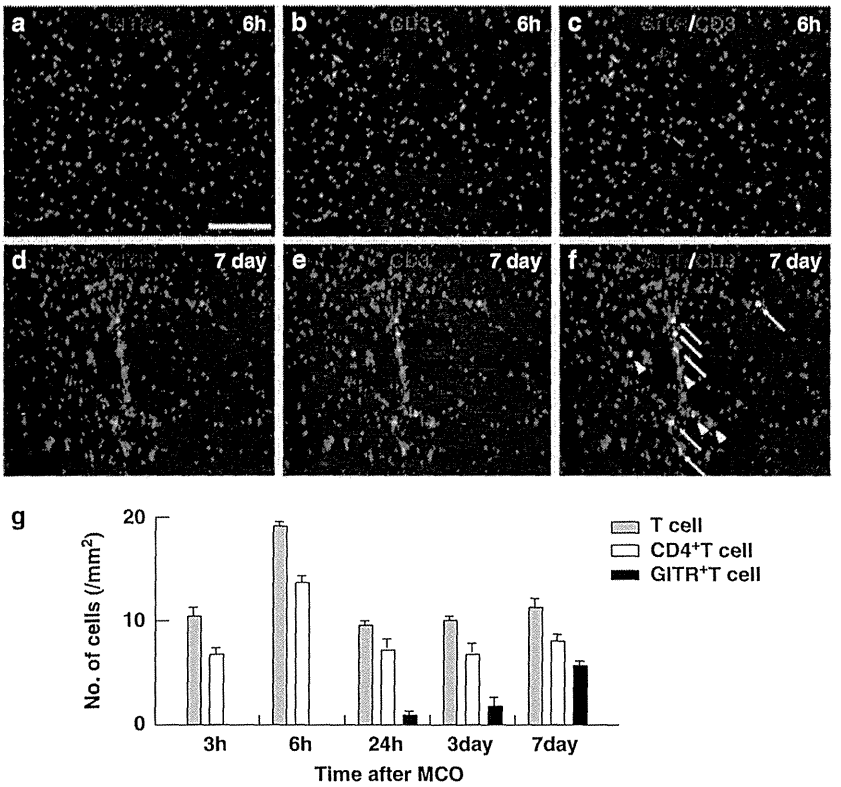

Figure 2 GITR-positive T-cell infiltration into the ischemic area of the poststroke brain. Immunohistochemistry for GITR$^+$T (**a–f**) cells infiltrated into the postischemic cortex 6 h (**a–c**) and 7 days (**d–f**) after stroke. The T cells were negative for GITR at 6 h (**a**: GITR; **b**: CD3; **c**: merged), but appeared to be positive for GITR at 7 days (arrows, **d**: GITR; **e**: CD3; **f**: merged). Arrowheads indicate GITR$^-$ T cells (**f**). (**a**) Scale bar: 100 μm. (**g**) Cells expressing CD3 (gray bars), CD4 (white bars) or GITR (black bars) 3 h, 6 h, 24 h, 3 days or 7 days after stroke were quantified. Results displayed are representative of three repetitions of the experimental protocol

CD4$^+$T cells. GITR was analyzed on CD3$^+$CD4$^+$ cells. No significant upregulation of CD25 on T cells was observed at days 1 and 7 after stroke (Figures 3c and e: 4.61% at day 1 and 4.06% at day 7). However, the percentage of GITR$^+$ T cells was increased from 6.17 to 86.50%, and the surface expression of GITR on CD4$^+$T cells at day 7 was significantly increased compared with that at day 1 (from 13.90 to 68.37 in mean channel value; Figures 3d and f), indicating enhanced expression of GITR as an activation marker for CD4$^+$T cells.

Effects of GITR triggering on cerebral infarction. Given that GITR triggering was involved in cerebral ischemic injury, we decided to examine whether stimulation or inhibition of GITR triggering affects cerebral infarction by using the same stroke model. Mice were treated with anti-GITR agonistic antibody (GITR–Ab: DTA-1), GITR–Fc fusion protein (blocking the GITR–GITRL interaction) or control IgG at 3 h and 3 days after stroke. The brain was then removed 30 days after stroke. The size of infarction in mice treated with GITR–Ab was apparently larger than that of mice treated with GITR–Fc (Figure 4a). Further analysis of the volume of each hemisphere based on brain sections demonstrated a significant decrease in the poststroke brain volume in GITR–Ab mice, and a significant increase in that of GITR–Fc mice, compared with control mice (Figure 4b). These findings indicated that ischemic injury was enhanced by GITR triggering, while ameliorated by its blocking.

Effects of GITR triggering on poststroke inflammation. We had until then attempted to determine how the triggering of GITR could affect poststroke inflammation. As several studies have reported that multiple cytokines modulate CNS inflammation,[2,3,19] the levels of IFN-γ, TNF-α and IL-10 were analyzed using quantitative real-time PCR in mice 7 days after stroke. The alteration of mRNA levels of these cytokines within the ischemic region was confirmed (Figure 4c–e). GITR–Ab treatment resulted in a significant elevation of IFN-γ ($P<0.05$) and TNF-α ($P<0.05$) levels, and a significant decrease in the IL-10 level ($P<0.01$) compared with the control IgG treatment. In contrast, treatment with GITR–Fc showed a significant decrease in IFN-γ ($P<0.01$) and TNF-α levels ($P<0.05$), and a significant increase in IL-10 level ($P<0.01$) compared with the control. These data indicated that GITR triggering largely affected cerebral ischemic injury by changing the level of poststroke inflammation (enhancing proinflammatory cytokines and suppressing anti-inflammatory cytokines).

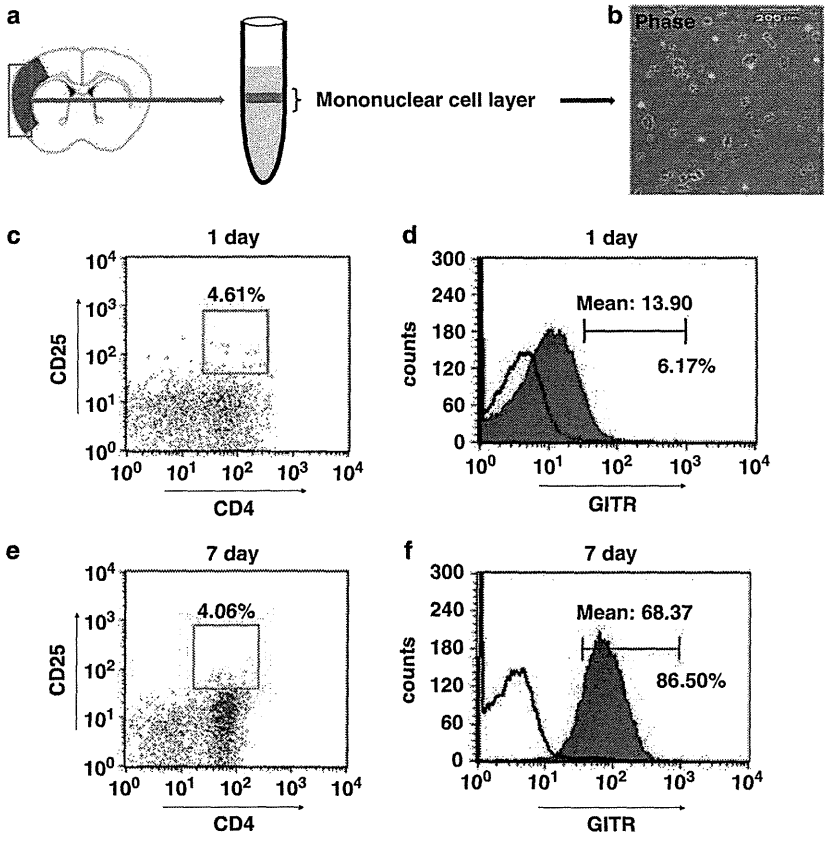

Figure 3 The analysis for the subpopulation of infiltrated cells in the ischemic area with FACS. (**a**) The ischemic tissue of the brain 7 days or 1 day after stroke was isolated and pressed through a cell strainer, and was separated by Ficoll-paque plus centrifugation. The extract contains lymphocyte-like mononuclear cells, which were observed under phase-contrast microscope. (**b**) FACS analysis for the subset of T cells that infiltrated the ischemic cortex was performed. The acquired lymphocytes were analyzed for $CD4^+$ and $CD25^+$ on $CD3^+$ cells 1 day (**c**) and 7 days (**e**), and for GITR on $CD3^+CD4^+$ cells 1 day (**d**) or 7 days (**f**) after stroke. The percentage of $CD25^+$ cells was evaluated in the total T cells ($CD3^+$ cells), and that of $GITR^+$ cells was evaluated in $CD4^+$ T ($CD3^+CD4^+$) cells extracted from the infarcted brain tissue. The mean channel values were displayed for GITR in the $CD3^+CD4^+$ cells. (**d** and **f**) Filled histogram represents GITR expression and open histogram represents isotype control

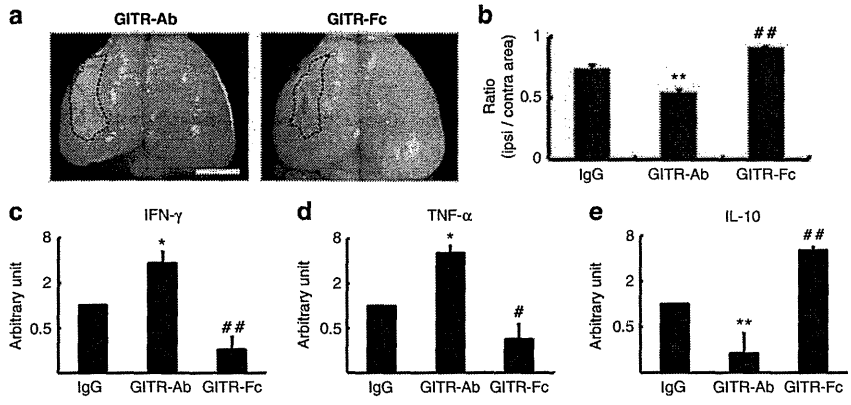

Figure 4 Effects of GITR triggering on the poststroke brain volume and cytokine expression. (**a**) On day 30 after stroke, brains of mice treated with either GITR-Ab or GITR-Fc were evaluated grossly. Areas of hatched line indicate infarct area. (**b**) Ipsilateral and contralateral cerebral hemisphere volume was calculated by integrating coronally oriented ipsilateral and contralateral cerebral hemisphere area. Involution of ipsilateral cerebral hemisphere volume calculated as (ipsilateral/contralateral cerebral hemisphere volume) confirmed a significant difference in brain volume in the poststroke hemisphere comparing the groups. (**b**) $n=5$ for each experimental group. (**a**) Scale bar: 2 mm. The expression of IFN-γ (**c**), TNF-α (**d**) and IL-10 (**e**) in the ischemic tissue on day 7 after stroke was detected by quantitative real-time PCR. The relative expression of mRNAs was represented as arbitrary unit, which was set at the level of the expression of the gene equal to 1 in the IgG-treated group using a logarithmic scale. The significance among the treatments was calculated from the relative level of mRNA expression. (**c–e**) $n=4$ for each experimental group. $^*P<0.05$ and $^{**}P<0.01$, GITR-Ab-treated mice *versus* control IgG-treated mice; $^{\#}P<0.05$ and $^{\#\#}P<0.01$, GITR-Fc-treated mice *versus* control IgG-treated mice

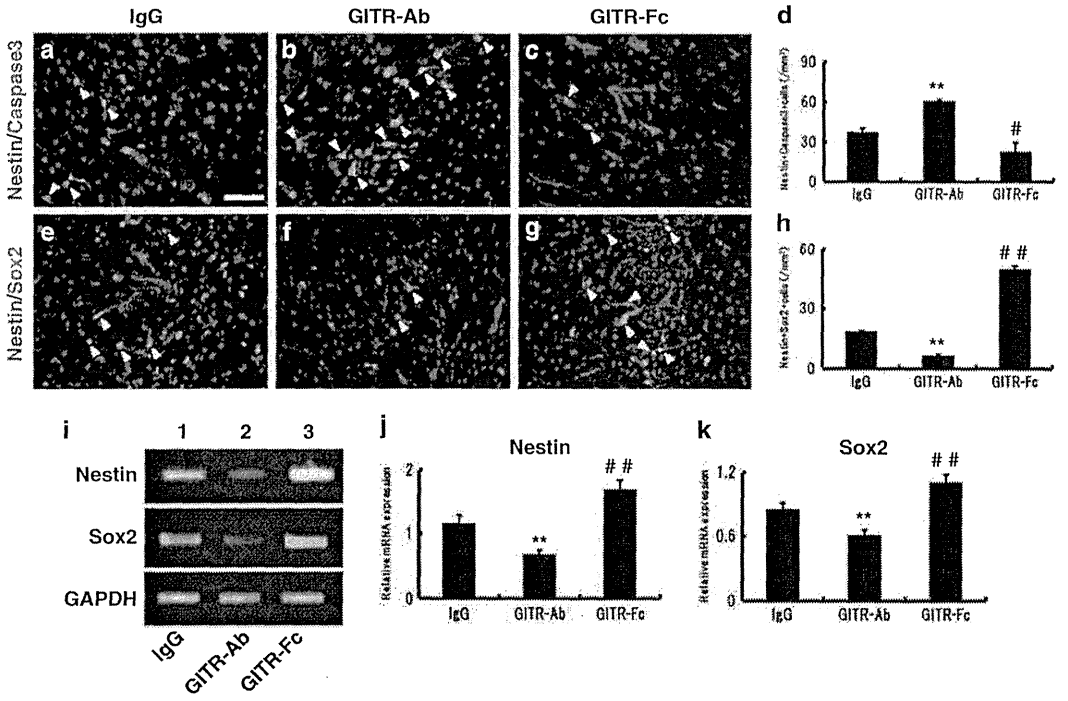

Figure 5 Effects of GITR–Ab or GITR–Fc on survival/death of neural stem/progenitor cells. (**a–d**) Co-expression of nestin (red) and active caspase-3 (green; arrowheads) was investigated 3 days after stroke at the border of the infarction. Compared with the control IgG-treated mice (**a**), GITR–Ab-treated mice showed an increased number of nestin/caspase-3-positive cells (**b**), whereas GITR–Fc-treated mice showed fewer co-expressing cells (**c**). (**e–h**) Co-expression of nestin (red) and Sox2 (green; arrowheads) was investigated 7 days after stroke. Few cells co-expressing nestin and Sox2 were observed in GITR–Ab-treated mice (**f**), whereas a number of nestin/Sox2-co-expressing cells were observed in GITR–Fc-treated mice (**g**). The number of nestin/caspase-3 cells (**d**) and nestin/Sox2 cells (**h**) at each period was significantly different on comparing the groups. (**d**) $n=3$ and (**h**) $n=4$ for each experimental group. (**i–k**) Expression of nestin or Sox2 was detected by conventional RT-PCR in the ischemic tissue on day 7 (**i**). Compared with the control IgG-treated mice (first lane), GITR-treated mice showed decreased expression of nestin or Sox2 (second lane), whereas GITR–Fc-treated mice showed increased expression (third lane). The relative expression was significantly different on comparing the groups (**j**: nestin; **k**: Sox2). (**j**) $n=4$ and (**k**) $n=5$ for each experimental group. (**a**) Scale bar: 100 μm. $^{**}P<0.01$, GITR–Ab-treated mice *versus* control IgG-treated mice; $^{\#}P<0.05$ and $^{\#\#}P<0.01$, GITR–Fc-treated mice *versus* control IgG-treated mice

Effects of GITR triggering on survival/death of neural stem/progenitor cells. Inflammation is known not only as a deteriorated factor of cerebral injury but also as a strong stimulator of neurogenesis. As the current study has proved that GITR triggering can regulate the inflammatory response,[15,17] we assessed the GITR–GITRL interaction, which may contribute to neurogenesis in the infarction area. Because we had previously showed that iNSPCs could contribute to poststroke neurogenesis and that cortical neurogenesis is related to the development of the iNSPCs,[8,20,21] the effects of GITR–Ab or GITR–Fc on survival/death of iNSPCs were investigated by using immunohistochemistry for nestin and active caspase-3 on the ischemic brain sections. The nestin-positive iNSPCs were observed at the border of the infarction as well as in the ischemic core 7 days after stroke (see Supplementary Figure 1B, red, nestin) as described.[6,8,20] Control IgG-treated mice appeared to have abundant nestin and active caspase-3 double-positive cells (Figure 5a, red, nestin; green, caspase-3). The administration of GITR–Ab increased the number of nestin/caspase-3 cells (Figure 5b), whereas that of GITR–Fc decreased it (Figure 5c). The number of activated caspase-3-positive iNSPCs was significantly different among the three groups (Figure 5d; $^{**}P<0.01$, GITR–Ab *versus* control IgG; $^{\#}P<0.05$, GITR–Fc *versus* control IgG). These findings indicate that GITR triggering induced, whereas its blocking suppressed, apoptosis of iNSPCs.

To provide further support for our hypothesis that GITR triggering participates in iNSPC-death/survival, expressions of nestin and Sox2 (SRY (sex determining region Y)-box 2), neural stem cells markers,[22] were assessed by immunohistochemistry (Figures 5e–h). Seven days after stroke, a number of nestin-positive cells express Sox2, especially at the border of infarction (Supplementary Figures 1A–D). The administration of GITR–Ab significantly decreased the number of nestin/Sox2 double-positive cells (Figures 5f and h; $P<0.01$ *versus* control IgG), whereas the administration of GITR–Fc increased them (Figures 5g and h; $P<0.01$ *versus* control IgG). These findings were confirmed by conventional reverse transcription (RT)-PCR (Figures 5i–k) using mRNA extracted from the infarcted cortex (Figure 5i). Relative expressions of nestin and Sox2 were attenuated by GITR–Ab treatment, and enhanced by GITR–Fc treatment (Figures 5j and k; $P<0.01$, among the three groups).